

5.1 Description of JEOL/Tracor Northern System

The SEM/microprobe system at the EERC consists of a JEOL 35U scanning electron microscope/microprobe, a GW Electronics backscattered electron detector, an ultrathin window energy-dispersive x-ray spectrometer, a wavelength-dispersive x-ray spectrometer, digital beam control, a Tracor-Northern 5600 x-ray microanalyzer control system, a Tracor-Northern 8500 image analyzer, and stage automation. The Tracor-Northern 5600 is interfaced with a personal computer system for advanced data manipulation and storage.

The key components of the SEM system that make it possible to image, size, and analyze inorganic particles include the backscattered electron detector, digital beam control, and the ultrathin window energy-dispersive x-ray spectrometer. The Tracor-Northern 8500 image analysis system can perform automated acquisition, storage, and processing of images from the SEM.

The CCSEM analysis technique uses backscattered electron imaging (BEI) and EDS to analyze minerals. Since the mineral or ash particles appear brighter in BEI relative to the lower atomic number background of the matrix, a distinction can be made between coal, epoxy, and mineral grains. Using the Tracor-Northern particle recognition and characterization program, the electron beam scans over the field of view to locate bright inclusions that correspond to mineral or ash species. On finding a bright inclusion, the beam performs eight diameter measurements on the inclusion, finds the center of the inclusion, and collects an EDS for 5 seconds. The system is configured to detect 12 elements: Na, Mg, Al, Si, P, S, Cl, K, Ca, Fe, Ba, and Ti. Data from the CCSEM analysis are transferred simultaneously to a personal computer where they are stored on disk. The following essential information for each particle analyzed is stored: size, area, perimeter, chemical composition (x-ray count percentages), coordinates of location on the sample surface, frame number, and number of energy-photon counts. Software developed at the EERC classifies the minerals into categories based on size and composition (20).

ADEM Description

In order to facilitate the development of fully automated SEM analysis routines using image analysis, an ADEM was purchased and is now in use. The Tracor Northern ADEM is the first SEM to obtain total system automation and computer control of all system parameters. The ADEM completely integrates analytical EDS and digital image processing (Figure 52). This totally automated and integrated system is being used for further developments in the CCSEM program. The JEOL/Tracor Northern system is not capable of changing beam parameters such as magnification, focus, and operating voltages in an automated, computer-controlled fashion. The control and monitoring of these parameters is integral for planned CCSEM developments outlined in the description of Subtask B, CCSEM Automation and Development. The ADEM provides further capabilities to the CCSEM development program because it is capable of the automated analysis of multiple samples, which greatly increases the efficiency of the entire system and the amount of beam time available for research and technique development. In addition, the ADEM is able to image objects as small as 0.1 μm in diameter, allowing analysis of the smallest ash particles.

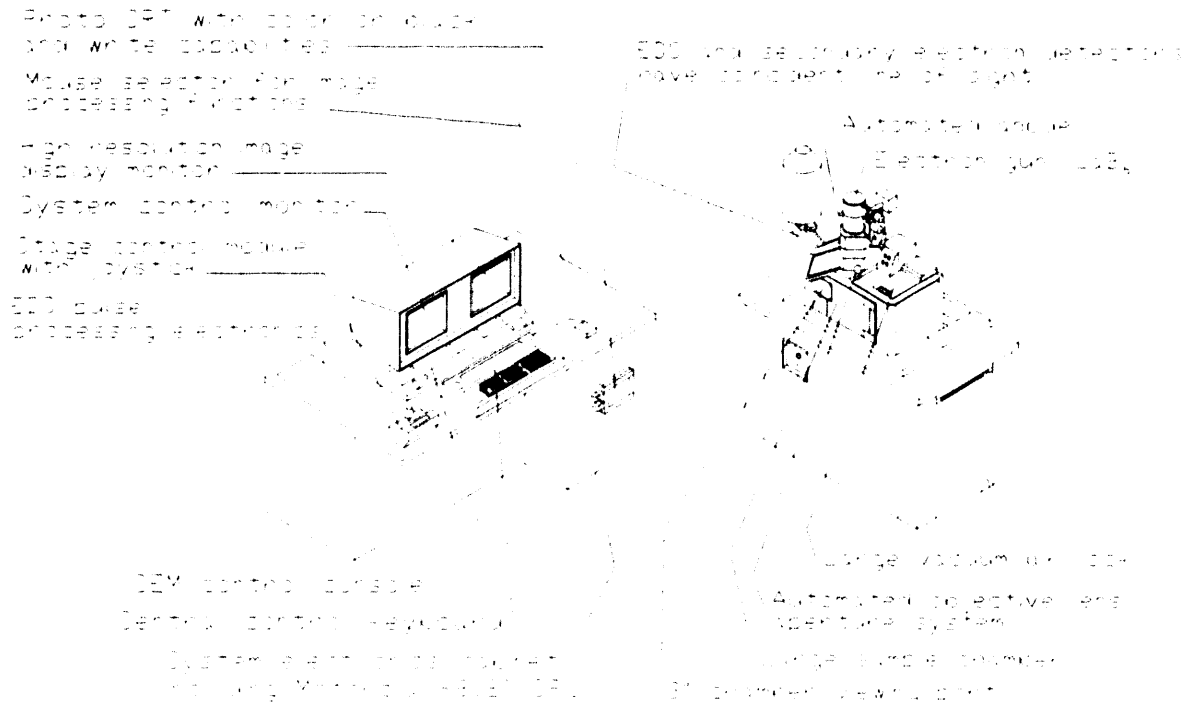


Figure 52. Tracor-Northern ADEM system.

5.2 Round-Robin CCSEM Analysis

5.2.1 Introduction

A round-robin study designed to investigate and evaluate the CCSEM method of quantitative coal mineral analysis is in progress. Polished epoxy mounts prepared from three Argonne Premium Coal Samples (23,24) are candidates for analysis by participating laboratories. The data obtained will be used to assess the performance characteristics of CCSEM and to optimize the method.

This effort was undertaken in response to the growing importance of CCSEM in coal mineral analysis. The scanning electron microscope (SEM) coupled with energy dispersive x-ray microanalysis is uniquely suited for coal mineral analysis because it provides both compositional and morphological information for individual particles. Manual operation of the analytical SEM has been used sparingly in coal mineral research because of the time required to acquire a statistically significant number of analyses to fully characterize the mineralogy of a coal sample. However, with the introduction of CCSEM (25-27), the time required to analyze a significant number of mineral particles has been greatly reduced. CCSEM is now a widely applied method for sizing, identifying, and quantifying coal mineral constituents. Quantitative coal mineral analysis and mineral size analysis are useful in characterizing the physical and chemical properties of coal; predicting the inorganic transformations that occur during combustion; and understanding the deposition, slagging, and fouling characteristics of combusted materials. Specific examples of recent CCSEM applications can be found in various publications (20,28-33).

Although CCSEM has been used extensively to analyze coal mineralogy, little information is available to evaluate the performance characteristics (i.e., precision, accuracy, sensitivity, and limitations) of this important analytical method. The evaluation process has been impeded because there are no certified coal mineral standards available, and there are only a limited number of laboratories employing CCSEM available to perform collaborative testing. Casuccio and others (34) and Vleeskens and Hamburg (35) conducted an interlaboratory testing study involving six laboratories to evaluate repeatability and reproducibility. The data from four of the participating laboratories were evaluated. Two of these participants used the same instrument and operating conditions. The authors attributed the majority of interlaboratory variability observed to differences in x-ray detector performance characteristics and backscattered electron (BSE) video threshold settings.

This report summarizes the objectives, organization, and plans of a round-robin testing study designed to investigate and evaluate the CCSEM method of quantitative coal mineral analysis. Argonne Premium Coal Samples Wyodak-Anderson, Illinois No. 6, and Pittsburgh No. 8 are potential candidates for analysis. Initial analyses will be performed by the EERC to ascertain the suitability of these coals for the round-robin testing. The data obtained will be used to optimize the method and to further develop a CCSEM procedure.

5.2.2 Background

5.2.2.1 General Description of the CCSEM Method

This section briefly describes the CCSEM procedures of collecting and presenting data that are common to the majority of laboratories participating in the study. Coals to be analyzed are mounted in a medium (e.g., epoxy, carnauba wax), cross-sectioned, polished, and carbon-coated. An SEM operating in the BSE imaging mode is programmed to scan preselected areas of the polished coal surface. Mineral particles are automatically detected by an increase in the BSE signal above a preset video threshold. The electron microbeam locates the center of the particle, measures its size, and collects an energy dispersive x-ray spectrum. Regions-of-interest in the spectra are defined to measure the characteristic x-ray emission intensities of common, mineral-forming, major and minor elements. The analyses are classified into various mineral categories, based on relative elemental intensities and stoichiometric criteria. The classified particles are allocated according to cross-sectional diameter into size intervals. The analysis is performed at different magnifications to provide the image resolution necessary to obtain information on the distribution of minerals in different size classes. The results are summarized in terms of the number and proportions of various mineral classification categories in their respective size intervals.

5.2.2.2 Factors Affecting CCSEM Results

Instrumentation characteristics, operating parameters, and procedures that are unique to the participating laboratories will affect the intra- and interlaboratory agreement of CCSEM analysis results. Critical factors are presented in Table 17. Many of these were identified and tabulated by Birk (36).

TABLE 17

Factors Affecting CCSEM Analysis Results of Coal

Coal Sample:	<ul style="list-style-type: none"> • Coal Heterogeneity • Coal Rank • Mineral Particle Size • Mineral Intergrowths • Representative Collection
Preparation:	<ul style="list-style-type: none"> • Comminution Method • Mounting Medium • Mounting Method • Polishing Method • Conductive Coating Method
Instrumentation:	<ul style="list-style-type: none"> • Operating Parameters (Beam Voltage/Current, Magnification, etc.) • Electron Beam Stability • Geometry (Working Distance, X-Ray Takeoff Angle, etc.) • X-Ray Detector Sensitivity and Efficiency • BSE Detector Sensitivity • Beam Control
Data Collection and Reduction:	<ul style="list-style-type: none"> • X-Ray Spectral Acquisition Time • Elements Analyzed • Magnification(s) • Number of Particles Analyzed per Mag. • Amount of Area Analyzed • Video-Sampling Signal Value • BSE Video Signal Threshold • Particle-Size Intervals • Mineral/Chemical Definitions • Classification Categories • Calculation Methods

In this study, the interlaboratory variability originating from coal sampling and preparation is virtually eliminated because all participating laboratories will analyze identically prepared samples. Samples were prepared, under the supervision of Dr. Paul Gottlieb of CSIRO, by mixing the coals with crushed graphite and epoxy, and then casting the mixture into 30-mm-diameter pellets. A major concern, however, is the variability resulting from differences in instrumentation performance characteristics, operating parameters, data acquisition parameters, and data reduction procedures. The experimental conditions routinely employed at various laboratories are summarized in Table 18.

5.2.3 Objectives and Organization of the CCSEM Round-Robin Study

5.2.3.1 Introduction

A three-task plan has been devised to achieve the objectives of this study (Table 19). The first task is designed to produce a database of

TABLE 18

CCSEM Experimental Conditions

Laboratory	Ames	EERC	KY	ECN	Sandia
Accelerating Voltage (kV)	15	15	20	20	15
Probe Current (nA)	0.7	0.6	0.7	0.6	variable
Magnifications (x)	50/200/500	50/240/500	20/100/500	50/150/450	50/200 or 300/500
Spectral Acquire Time (sec)	3	5	2	2	10
SEM	JEOL 840A	JEOL JSM-35	ETEC- Autoscan	JEOL 840	JEOL 733 or JEOL JSM-35
X-Ray Analyzer	KeveX Delta-V	TN-5500	TN-2000	TN-2000	TN-5502
Software	KeveX Feature Analysis, LeMont Scientific Line Scan Analysis	PRC* PartChar ^{©**}	CMA*	CMA	CMA PRC

* Coal Mineral Analysis and Particle Recognition and Characterization computer programs marketed by NORAN Instruments, Inc. (formally Tracor Northern) (37).

** Particle Characterization computer program developed by the Energy and Environmental Research Center.

TABLE 19

CCSEM Round-Robin Task Objectives

Task 1: Initial CCSEM Round-Robin Testing

Compile a database of interlaboratory CCSEM analyses acquired on identical coal samples using documented analysis parameters and procedures.

Task 2: Evaluation and Investigation of the Round-Robin Analysis Results

- (a) Identify sources of intra- and interlaboratory variability.
- (b) Develop a CCSEM procedure for quantifying coal mineralogy based on recommendations accepted by a consensus of the round-robin participants.
- (c) Assess the performance characteristics (i.e., repeatability and reproducibility) of the CCSEM method.

Task 3: Reporting of CCSEM Round-Robin Test Study

Prepare a final report summarizing the CCSEM round-robin test results and recommendations of the participants.

interlaboratory CCSEM analysis results collected under very general guidelines. The seven laboratories identified above are anticipated to contribute to this database. In the second task, a CCSEM procedure will be developed based on a detailed analysis of the round-robin database in conjunction with the recommendations of participants. The third task involves the reporting of results and recommendations of the round-robin study. These tasks are subdivided into subtasks and described in the subsequent sections of this report.

5.2.3.2 Contacted Personnel and Laboratories

Dr. Harry ten Brink and Dr. G. Hamburg, Netherlands Energy Research Foundation ECN, 1755 ZG Petten, The Netherlands, Telephone: 31-2-246-3489, Fax: 31-2-246-4480.

Dr. Gary Casuccio, R.J. Lee Group, Monroeville, PA 15146, USA, Telephone: (412) 325-1776, Fax: (412) 733-1799.

Dr. Paul Gottlieb, CSIRO Division of Mineral & Process Engineering, Clayton, Victoria 3168, Australia, Telephone: 61-3-541-1222, Fax: 61-3-562-8919.

Dr. Gerry Huffman, University of Kentucky, Lexington, KY 40506, USA, Telephone: (606) 257-4027, Fax: (606) 258-1049.

Dr. Warren Straszheim, Ames Laboratory, Institute for Physical Research & Technology, Iowa State University, Ames, IA 50011, USA, Telephone: (515) 294-8187, Fax: (515) 294-3091.

Dr. Nancy Yang, Sandia National Laboratories, Combustion Research Facility, Livermore, CA 94550, USA, Telephone: (510) 294-2680, Fax: (501) 294-1004.

Mr. Chris Zygarlicke, Energy & Environmental Research Center (EERC), University of North Dakota, Grand Forks, ND 58202, USA, Telephone: (701) 777-5000, Fax: (701) 777-5181.

5.2.3.3 Task 1: CCSEM Round-Robin Testing

5.2.3.3.1 Sample Description, Preparation, and Distribution

Ampules of 100-mesh Wyodak-Anderson subbituminous coal, Illinois No. 6 high-volatile bituminous coal, and Pittsburgh No. 8 high volatile bituminous coal were obtained from the Argonne Premium Coal Sample Program. Argonne Premium Coal Samples were selected because their physical and chemical properties are well characterized (23,24,28,38-41). Samples were prepared, under the supervision of Dr. Paul Gottlieb of CSIRO, by mixing the coals with crushed graphite and epoxy, and then casting the mixture into 30-mm-diameter pellets. The sample surfaces were polished and coated with a thin conductive layer of carbon. A total of five CCSEM analyses will be performed by each participating laboratory on the three coals (Table 20). A polished epoxy mount of the Illinois No. 6 coal and the Wyodak-Anderson coal will be routed to each participating laboratory according to the schedule in Table 21. Participants will also receive an epoxy mount of the Pittsburgh No. 8 coal. The EERC will analyze these coals initially to determine their suitability for the round-robin study.

5.2.3.3.2 Analysis Guidelines

The information in Tables 17 and 18 was used to formulate analysis guidelines for the tests, as listed in Table 22. The analyses are to be performed at three magnifications of 500x, 240x, and 50x corresponding to particle diameter range limits of 1.0-4.6 μm , 4.6-22 μm , and 22-100 μm , respectively, with at least 1000 particles analyzed at each magnification, or

TABLE 20

Round-Robin Test Matrix

Coal	Sample Identification	Laboratory	Number of Analyses
Illinois No. 6	COLH064D	All	1
Wyodak-Anderson	COLH063D	All	1
Pittsburgh No. 8	COLH062F	Ames	3
"	COLH062C	CSIRO	3
"	COLH062E	ECN	3
"	COLH062D	EERC	3
"	COLH062G	Kentucky	3
"	COLH062H	Sandia	3
"	COLH062B	R.J. Lee	3

TABLE 21

Sample Distribution and Analysis Schedule		
Suggested Sample Receiving Dates and Analysis Reporting Dates		
Laboratory	Pittsburgh No. 8 Coal	Illinois No. 6 and Wyodak-Anderson Coals
EERC	June 8 - July 8, 1992	June 1 - June 14, 1992
ECN	June 8 - July 8, 1992	June 15 - June 29, 1992
Ames	June 8 - July 8, 1992	June 30 - July 14, 1992
Kentucky	June 8 - July 8, 1992	July 15 - July 29, 1992
R.J. Lee	June 8 - July 8, 1992	July 30 - August 13, 1992
CSIRO	June 8 - July 8, 1992	August 14 - August 28, 1992
Sandia	June 8 - July 8, 1992	August 31 - Sept. 14, 1992

Note: After completing the analyses, the laboratories will immediately return the samples to Mr. Chris Zygarlicke, Energy and Environmental Research Center, University of North Dakota, Box 8213, University Station, Grand Forks, ND 58202.

TABLE 22

Round-Robin CCSEM Analysis Guidelines	
Operating Parameters:	
Accelerating Voltage (kV)	15 or 20
Probe Current (nA)	N.S.*
Magnifications (x)	50/240/500
Data Acquisition Parameters:	
Number of Particles Analyzed per Magnification	1000
Particle Diameter Range Limits (μm)	1.0-4.6 @ 500x 4.6-22 @ 240x 22-100 @ 50x
Spectral Acquisition Time (sec)	2-10
Video Sampling Signal (Dimensionless Quantity)	N.S.
BSE Video Threshold (Dimensionless Quantity)	N.S.
Data Reduction Parameters:	
Classification Categories	N.S.
Category Definitions	N.S.
Particle-Size Intervals	N.S.

* Not specified.

until the entire sample is analyzed. These operating and data acquisition guidelines are specifically designed for the quantitative analysis of mineral particles as small as one micron in diameter. The implementation of these guidelines will reduce interlaboratory variability resulting from differences in operating parameters, data acquisition parameters, and counting statistics. Critical parameters that are not specified are the BSE video threshold setting and the video sampling signal value.

5.2.3.3.3 Analysis Reporting Requirements

The intra- and interlaboratory agreement of CCSEM results will be assessed based on the measured area fractions of individual mineral/chemical classification categories. Specific information about critical operating, data acquisition, and data reduction procedures must also be reported by each participant to facilitate the investigation of the method and the interlaboratory comparison of results. The minimum requirements for reporting each analysis are as follows:

1. Information enumerated in Table 22.
2. Analysis report containing information on the measured area fractions of individual mineral/chemical classification categories.
3. A data file saved to computer disk (3½" or 5¼" disk), preferably in ASCII format, containing the following analysis information on a particle-by-particle basis:
 - a. Particle number (1, 2, 3...) corresponding to the order in which a particle was analyzed.
 - b. Total x-ray counts acquired for the particle.
 - c. Elemental (Na, Mg, Al, Si...) relative intensity percents calculated by dividing the net counts for each element's spectral region-of-interest by the total x-ray counts and multiplying by 100.
 - d. Average cross-sectional particle diameter (μm).
 - e. Calculated cross-sectional particle area (μm^2).
 - f. Frame number corresponding to the image area that the particle was located in during analysis.
4. Total area imaged (μm^2) per frame on the sample at each magnification.

This information and the five CCSEM analyses must be completed and sent to Mr. Chris Zygarlicke or Mr. Kevin Galbreath of the EERC for processing according to the schedule in Table 21.

5.2.3.4 Task 2: Evaluation and Investigation of the Round-Robin Analysis Results

5.2.3.4.1 Introduction

Data from the test will be compiled and statistically analyzed to provide a measure of the intra- and interlaboratory agreement of CCSEM results. The statistical analysis will provide a quantitative basis for

judging the general performance capability of CCSEM. The compiled data will also be used to investigate possible sources of intra- and interlaboratory variability. After identifying the factors that contribute to the variability, improvements will be made to CCSEM procedures.

5.2.3.4.2 Standardization of CCSEM Data Reduction

Interlaboratory comparison of the analysis results will be hindered because of differences in data reduction routines. Data reduction involves the classification of the particle analyses into various user-specified mineral categories and size intervals. The classification categories are defined based on elemental relative intensities, relative intensity ratios, and stoichiometric criteria. The categories, category definitions, and size intervals are inconsistent among the participating laboratories.

Information supplied by the participating laboratories will be used to develop a standard data reduction/classification routine that will sufficiently characterize the major mineralogy of most coals. Data from each laboratory will be reprocessed with the standard classification routine. By processing the data through a standardized data reduction program, the direct comparison of analysis results will be possible.

5.2.3.4.3 Recommended CCSEM Procedure

A CCSEM procedure will be drafted, based on a thorough review of the initial round-robin analysis parameters and procedures.

5.2.3.5 Task 3: Reporting of CCSEM Round-Robin Test Study

5.2.3.5.1 Information Dissemination

A quarterly newsletter will be sent to participating laboratories. The newsletter will provide current information about the study's progress and will also serve as a forum for participants.

5.2.3.5.2 Report Preparation

A final report will be prepared summarizing the CCSEM round-robin test results and recommendations of the participants. Included in this report will be a detailed description of the recommended procedure and a formal statement regarding the performance characteristics (i.e., repeatability and reproducibility) of the CCSEM method.

5.2.3.6 Proposed Additional Round-Robin Testing

If warranted, an additional round-robin test could be performed to verify the procedure's usefulness and to identify technical weaknesses. This additional test should be conducted according to an internationally acceptable protocol designed following the guidelines of an appropriate professional society (42-44).

5.2.3.7 CCSEM Round-Robin Schedule

The round-robin study of the CCSEM method of coal mineral analysis will proceed according to the schedule in Table 23. The EERC is responsible for

TABLE 23

CCSEM Round-Robin Schedule

Tasks and Subtasks	1992			1993	
	Apr-Jun	Jul-Sep	Oct-Dec	Jan-Mar	Apr-Jun
Task 1: CCSEM Round-Robin Testing	←-----→				
1.1 Sample Distribution	0	0 0 0			
1.2 Acquisition of Test Data	X	X X X			
1.3 Data Compilation			0		
Task 2: Evaluation and Investigation of the Round-Robin Analysis Results	←-----→				
2.1 Statistical Analysis of Test Results			0 0		
2.2 Investigation of Intra- and Interlaboratory Variability			0	0	
2.3 Meeting to Discuss Test Data and Identify Future Directions				X	
2.4 Standardization of CCSEM Data Reduction				X X	X
2.5 Development of a CCSEM Procedure				X X	X
Task 3: Reporting of CCSEM Round-Robin Test Study	←-----→				
3.1 Preparation and Distribution of Quarterly Newsletter		0	0	0	0
3.2 Preparation of Final Report					X X

X = Responsibility of all the round-robin participants.

0 = Responsibility of the Energy & Environmental Research Center.

completing Subtasks 1.1, 1.3, 2.1, 2.2, and 3.1. The involvement of all the round-robin participants is required to complete Subtasks 1.2, 2.3, 2.4, 2.5, and 3.2.

5.3 ZAF Correction of CCSEM Data

A ZAF procedure for the CCSEM routine was made possible by an off-line correction program received from the University of California-Berkeley. This program can be run on a personal computer (PC) in a fraction of the time needed to complete the corrections on-line. The primary reason ZAF corrections were not previously made was because a large amount of time was needed to process the data on the SEM computer. The program requires the k-ratios as measured using integrated counts obtained from the x-ray spectra. The current Particle Recognition and Characterization (PRC) (Tracor Northern) program was modified to produce both the EDS elemental percentages, as before, along with the k-ratios. This requires slightly more time, but is believed to be worth the extra time to retain the capability of comparing data in both forms. The k-ratios are then ZAF-corrected using the PC-based program. This new data format will necessitate modifications to the mineral classification scheme.

To date five ashes and three coals have been used to test the ZAF correction program. The tests were designed to compare the bulk major elemental composition of the coals as determined using both CCSEM with ZAF corrections, and x-ray fluorescence (XRF). X-ray fluorescence is well-established as an ASTM-certified method, and so these data are considered to be reliable as standards for comparison with the new CCSEM-ZAF results. Scanning electron microscope point count (SEMPC) data, when available, are also used for comparison.

CCSEM-ZAF data for five different ash samples were first considered. The samples include two of 100% Wyoming coal ash, and three of ash from a 70/30 blend of Wyoming and Oklahoma coals. For each sample, data obtained using CCSEM-ZAF were compared with XRF and SEMPC results. Bulk compositions, shown in Figure 53 through 57, were measured directly using XRF, and were calculated from particle-by-particle and point-by-point data for the CCSEM-ZAF and SEMPC data, respectively.

Sample #2 of the 100% Wyoming ash (Figure 54) and all three of the blend ash samples (Figures 55 through 57) indicate similar deficiencies for the CCSEM-ZAF data: weight percentages of Fe_2O_3 and CaO are too high and those of MgO , Al_2O_3 , and SiO_2 are too low. The XRF and SEMPC results for the ash samples are in close agreement. The overrepresentation of Fe_2O_3 in the CCSEM-ZAF data sets may be caused by the exceptionally high brightness of Fe-bearing materials in the images used by the SEM (26). MgO , Al_2O_3 , and SiO_2 may be present partially as submicron and organically bound material, and thus not detected using CCSEM. CCSEM-ZAF results for sample #1 of the 100% Wyoming ash (Figure 53) indicate generally opposite trends than those of the other four samples; this particular CCSEM-ZAF analysis may be biased by the inclusion of an unusually high proportion of large particles in the data set.

Three bituminous coals were also used for ZAF testing. CCSEM-ZAF results for Island Creek, Jader, and Kentucky #9 coals were converted to bulk compositions for comparison with XRF data, as shown in Figures 58, 59, and 60.

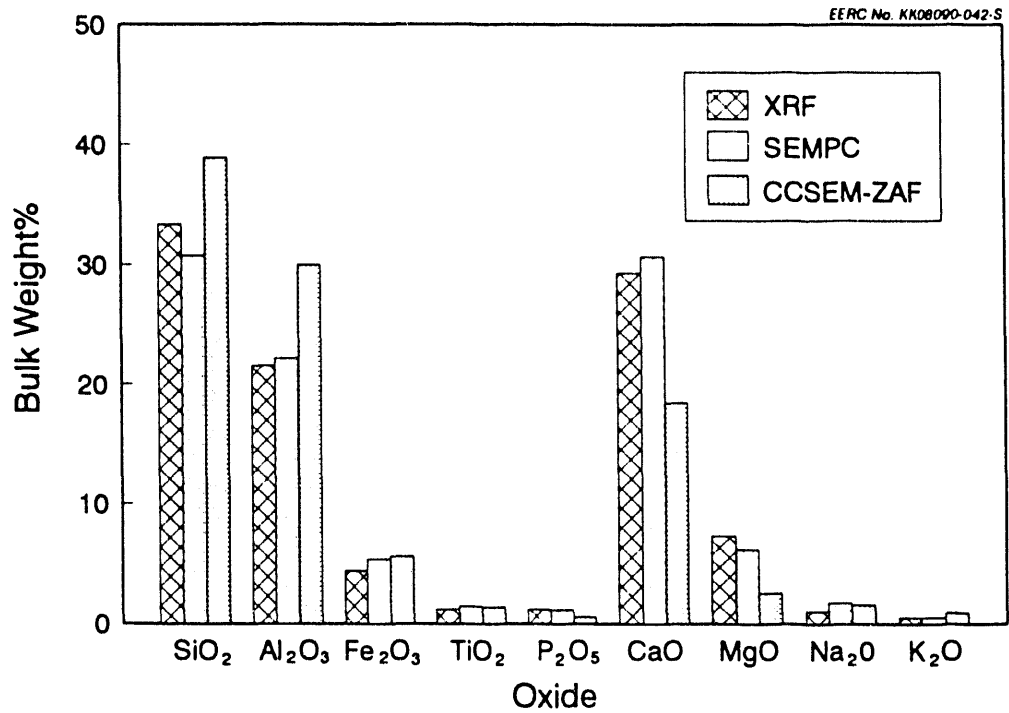


Figure 53. Bulk composition (SO_3 -free) for 100% Wyoming ash, Sample #1, as determined using XRF, SEMPC, and CCSEM-ZAF.

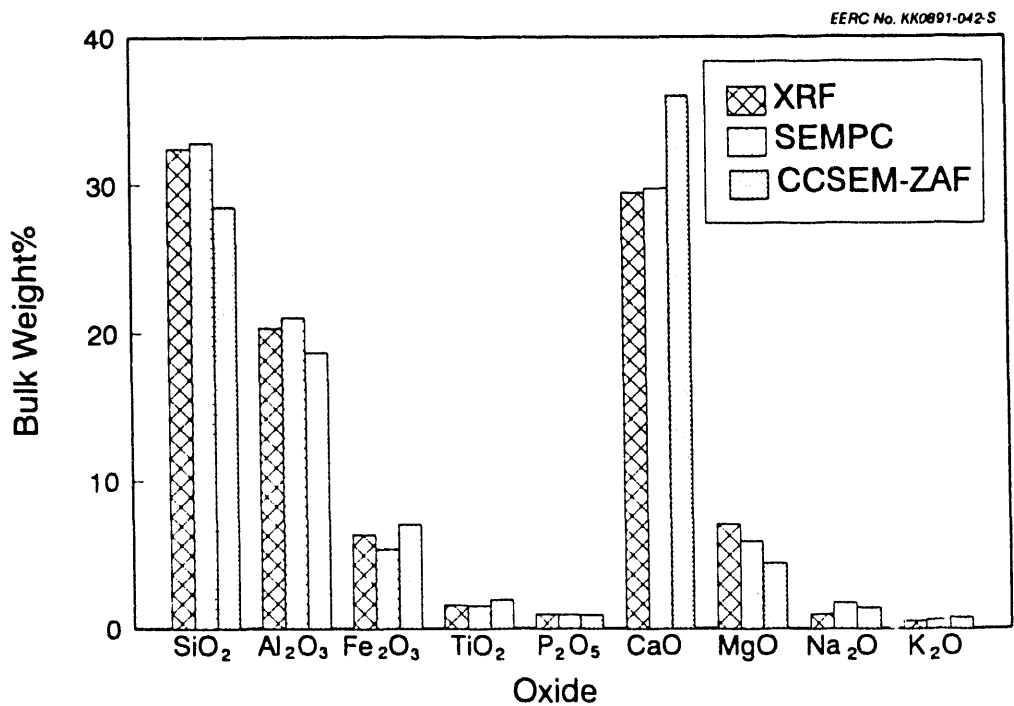


Figure 54. Bulk composition (SO_3 -free) for 100% Wyoming ash, Sample #2, as determined using XRF, SEMPC, and CCSEM-ZAF.

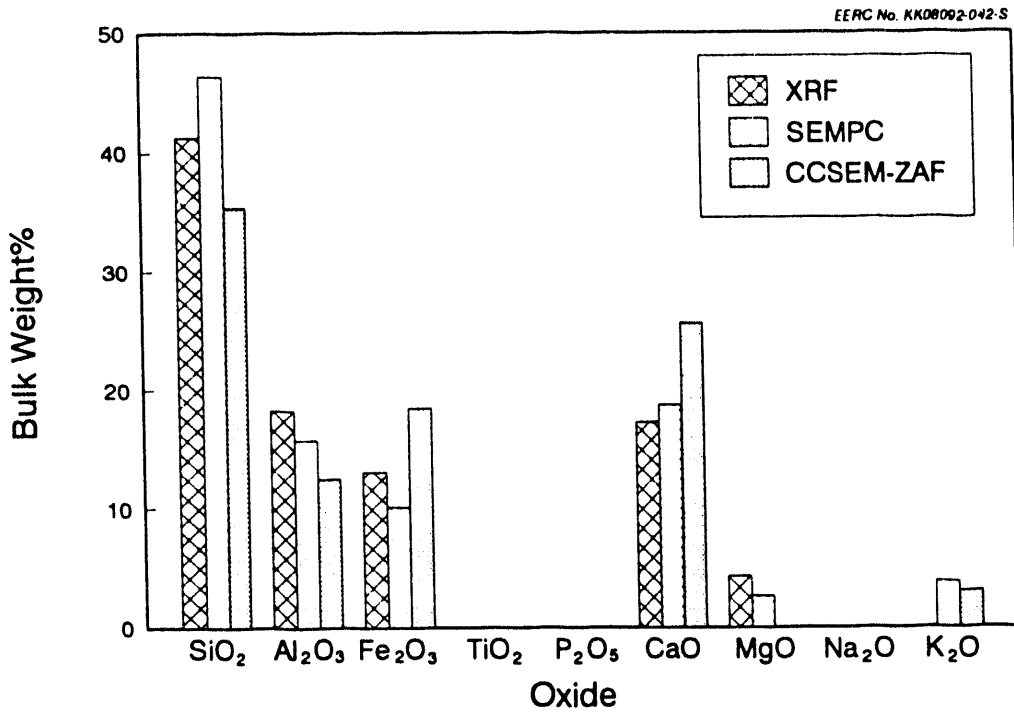


Figure 55. Bulk composition (SO₃-free) for Wyoming/Oklahoma blend ash, Sample #1, as determined using XRF, SEMPC, and CCSEM-ZAF.

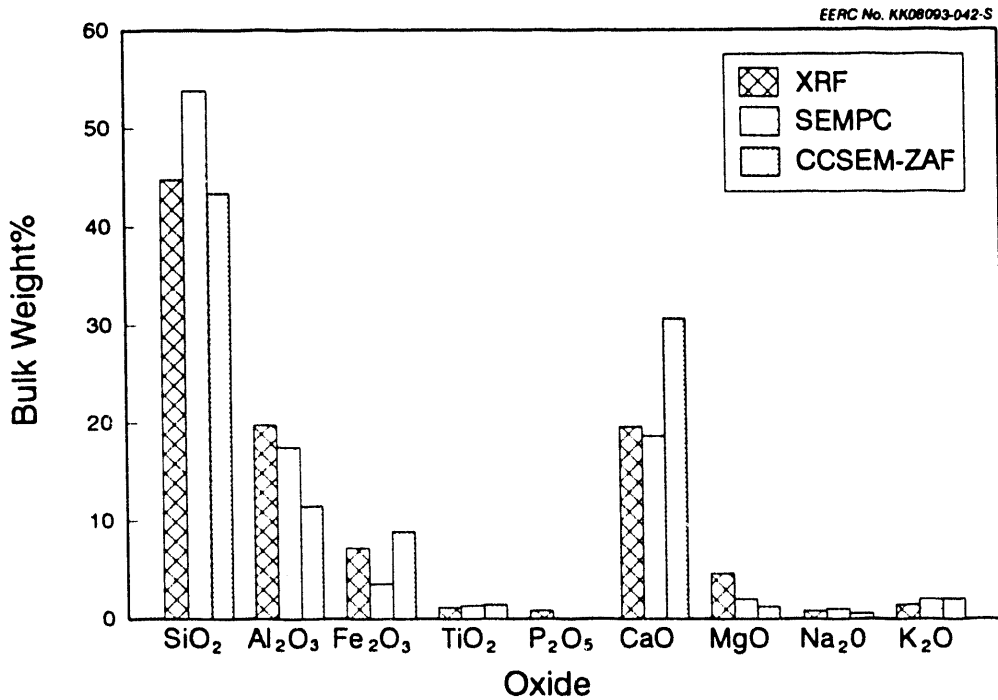


Figure 56. Bulk composition (SO₃-free) for Wyoming/Oklahoma blend ash, Sample #2, as determined using XRF, SEMPC, and CCSEM-ZAF.

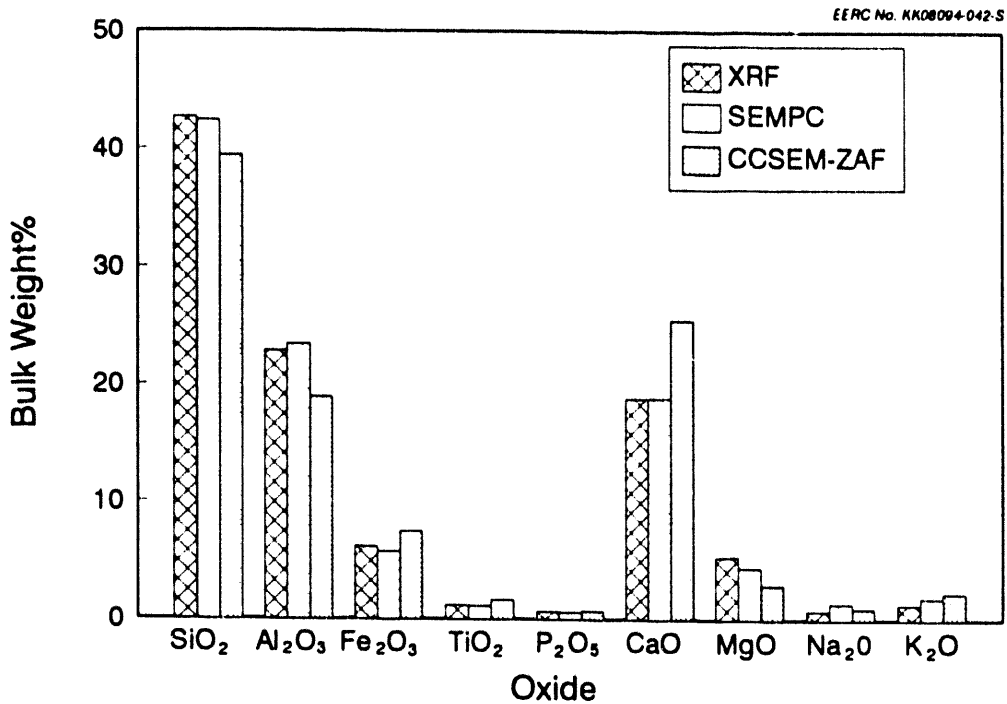


Figure 57. Bulk composition (SO₃-free) for Wyoming/Oklahoma blend ash, Sample #3, as determined using XRF, SEMPC, and CCSEM-ZAF.

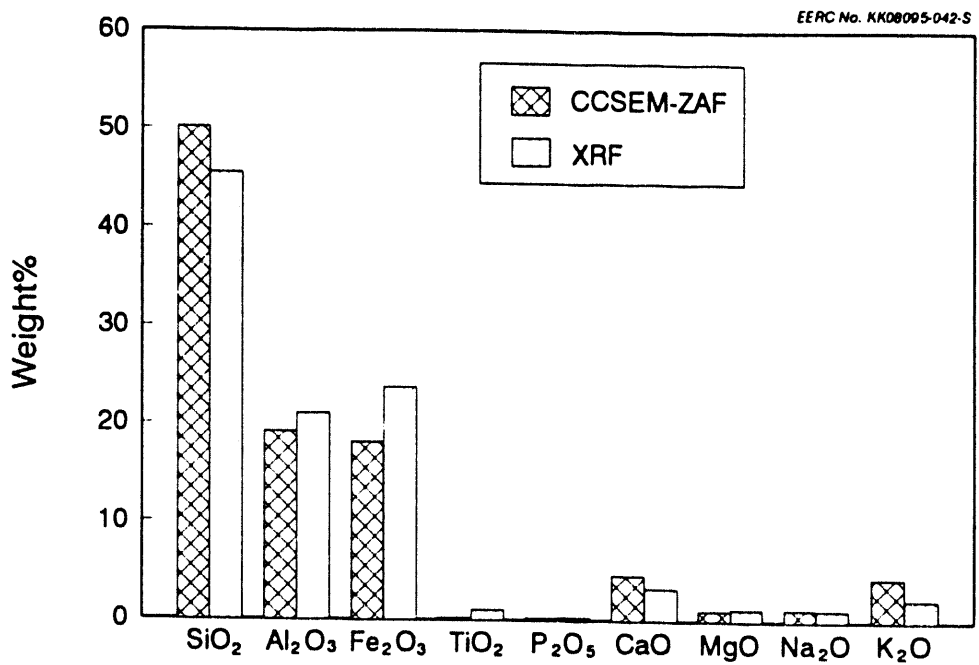


Figure 58. Bulk compositions (SO₃-free) for Island Creek coal, as determined using CCSEM-ZAF and XRF.

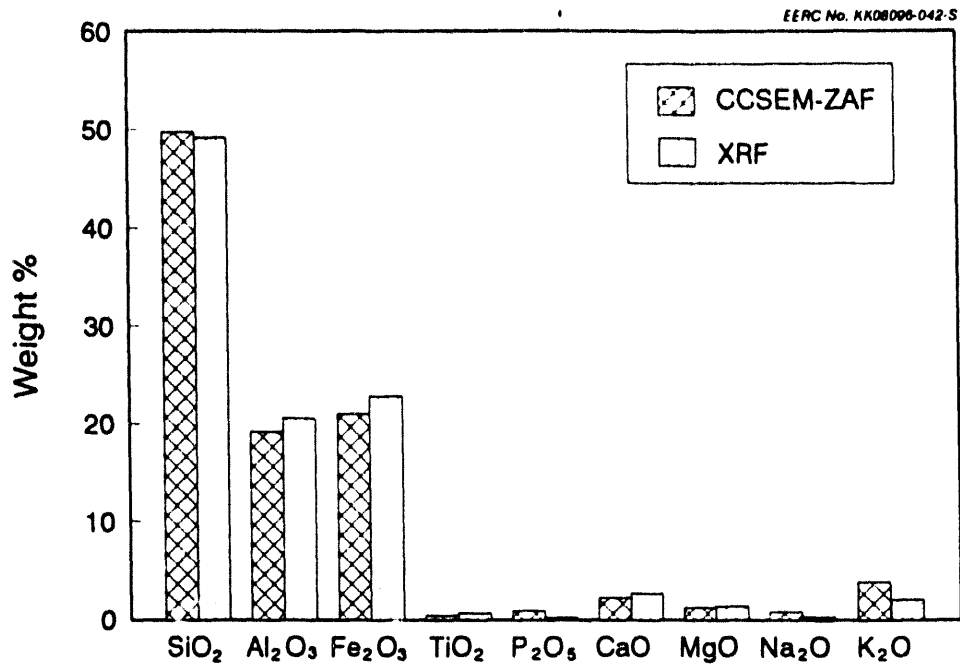


Figure 59. Bulk compositions (SO₃-free) for Jader coal, as determined using CCSEM-ZAF and XRF.

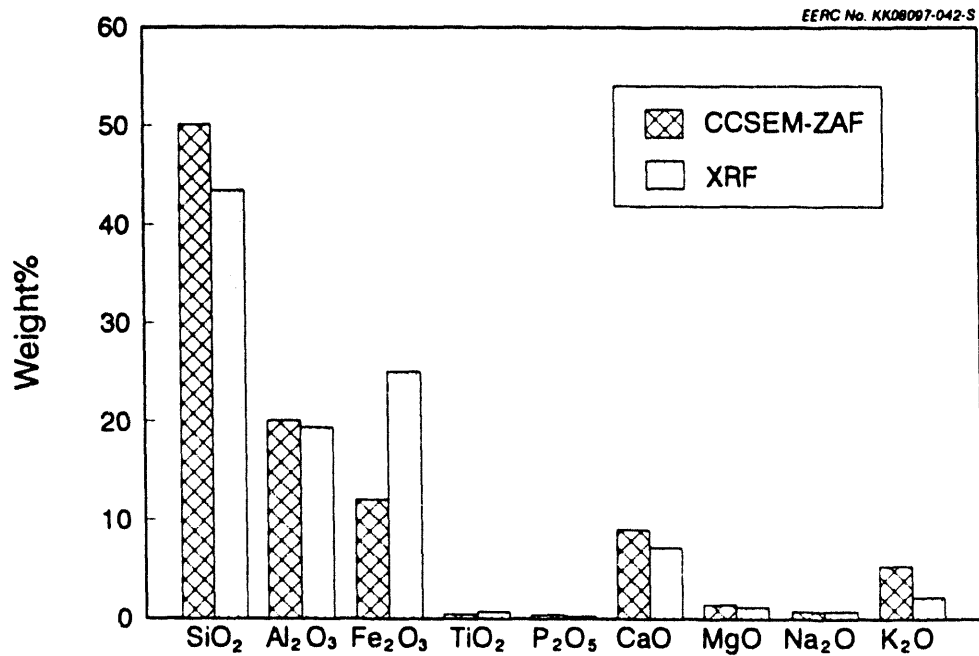


Figure 60. Bulk compositions (SO₃-free) for Kentucky #9 coal, as determined using CCSEM-ZAF and XRF.

Results are consistent among the three coals, but differ from results for the five ash samples discussed above. For the coals, SiO_2 and K_2O are slightly too high in the CCSEM-ZAF results and too low for Fe_2O_3 . It is not yet clear why the coal and ash samples yielded different trends in the CCSEM-ZAF testing. This issue will be resolved as more analyses are completed as part of ongoing projects. Advances in mass balancing and analysis of submicron particles will be applied to the CCSEM-ZAF results to improve the procedure as more samples are analyzed.

5.4 Particle-by-Particle Scanning Electron Microscopy (PBPSEM)

5.4.1 Introduction

The physical and chemical properties of minerals that control their behavior during coal combustion and ash deposition include size, composition, identity, relative abundance, and degree of association with the organic matrix. Therefore, knowledge of these parameters should facilitate the prediction of mineralogical transformations associated with coal combustion and ash deposition. In recent years, methods employing an automated scanning electron microscope (SEM) have been developed and applied at the EERC for obtaining this important information (20,33). This work has focused primarily on determining the size distribution of minerals in coal and quantifying the mineralogical composition of coal. Currently, our efforts are focused on developing and applying digital image processing and analysis techniques in conjunction with SEM for quantifying the association of mineral grains with the organic coal matrix.

Most SEM digital image processing and analysis systems provide algorithms for acquiring the required morphological data for such an analysis. These algorithms are based on the image segmentation process of transforming an original gray-scale image into a binary image. This process requires operator intervention to select gray-level thresholds for segmenting the coal and mineral phases from the image. Unfortunately, this can be very time consuming and involves subjective judgement by the operator to create binary images that accurately represent the original image. An automatic threshold selection algorithm was formulated and incorporated into an image analysis application program to increase the efficiency of acquiring morphological data and to enhance the objectivity of analysis results (45). The program completely automates digital image acquisition, processing, and image segmentation.

The particle-by-particle scanning electron microscopy (PBPSEM) method, described in this report, integrates this automated SEM image analysis capability with the well-established electron-probe microanalysis technique to measure various morphological and compositional parameters for individual mineral grains in coal. These data are compiled and classified according to compositional criteria into various mineral/chemical categories using a modified version of the Particle Characterization (PARTCHAR) program (20). The program provides a complete statistical summary of the results for all the mineral/chemical phases in a sample, including the proportion of each phase directly associated with coal.

5.4.2 Description of the PBPSEM Method

5.4.2.1 Sample Preparation and Instrumentation

Coals to be analyzed by PBPSEM are pulverized to a standard combustion grind (i.e., approximately 80% of the particles -200 mesh), mounted in carnauba wax (46), cross sectioned, and polished using standard petrographic procedures (47). Samples are then sputter-coated with carbon to minimize electron-beam charging artifacts. A JEOL JSM-35 SEM equipped with a NORAN Instruments (formally Tracor Northern, TN) Micro-Z ultrathin window x-ray detector, TN-5500 x-ray analyzer, TN-5600 stage automation system, TN-8500 image analyzer, and GW Electronics annular solid-state backscattered electron (BSE) detector is utilized for performing PBPSEM analyses.

5.4.2.2 Digital Image Acquisition, Processing, and Analysis

The SEM, operating in the BSE imaging mode, is programmed to analyze preselected areas on the sample. The electron microbeam is rastered across the analysis areas to acquire digital images at a spatial resolution of 512 pixels in both the line-scan (x-) and frame-scan (y-) directions. Frame averaging is employed to enhance image quality.

The PBPSEM routine first acquires a backscattered electron image (BEI). Backscattered electron imaging is used because the production of the backscattered electrons is a function of the average atomic number of the materials under the electron beam. The image produced by the detector will have varying grey scales representing the different chemical compositions in the sample. Areas rich in high atomic number elements will appear much brighter than areas of low average atomic number. Thus in coals, where the average atomic number of the carbonaceous matrix is approximately 6, the mineral phases will be easily identified as their average atomic number is far greater than 6.

A modified version of NORAN Instruments Locked and Liberated image analysis program (48) is used to locate particles and measure various morphological, phase correlation, and compositional parameters. Coal and mineral particles are delineated based on the atomic number contrast inherent in BSE imaging (49). An automatic threshold selection algorithm segments the coal and mineral phases from the gray-scale BSE image into separate binary images (45). The selection algorithm utilizes the image's gray-level histogram. Gray-level histograms of prepared coal samples are generally bimodal consisting of two peaks corresponding to the average brightness (i.e., mean atomic number) of mounting medium and coal, a valley that separates the peaks and represents the less heavily populated intermediate gray levels of coal particle edges, and an essentially featureless region corresponding to a large range in mineral gray-level intensity as a result of compositional variation. In some coal samples, the mounting medium and coal peaks are poorly resolved and the selection algorithm has difficulty in locating the histogram valley separating the two peaks (Figure 61a). A median filter is applied to the image to create a more strongly bimodal histogram (Figure 61b). The filtered histogram facilitates the selection of thresholds by the method described in this section. The median filter was chosen because it suppresses digital image noise without significantly affecting particle edges or other image features (50). The automatic threshold selection algorithm searches for the mounting medium and coal peaks and then selects a threshold at the minimum

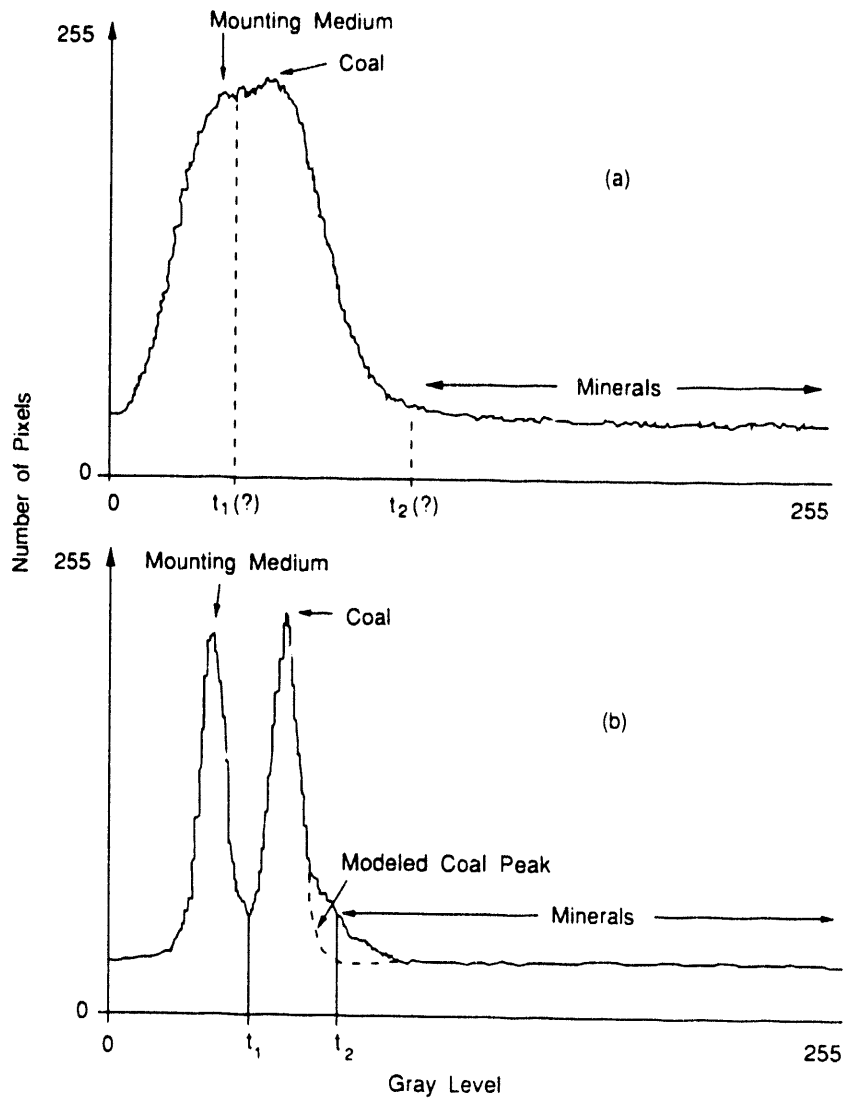


Figure 61. Grey-level histograms, (a) original histogram, the selection of thresholds segmenting mounting medium from coal (t_1) and coal from minerals (t_2) is arbitrary; (b) median-filtered histogram (5 x 5 filter), mounting medium and coal peaks are resolved, thus facilitating automatic threshold selection by the method described in the text.

intensity value in the histogram valley (Figure 61b). This method of threshold selection is referred to as the mode method or standard histogram method (51,52). The threshold segments coal from the mounting medium. Another threshold is selected to segment the coal from minerals. The placement of this threshold involves a peak modeling procedure to account for any asymmetry of the coal peak caused by the overlapping of coal and mineral gray levels. The procedure models the coal peak assuming a Gaussian distribution of gray levels and then establishes a threshold at the base of the modeled peak (Figure 61b). Thresholds are determined for each analysis area on the sample to compensate for instrument drift.

After transforming the gray-scale image into coal and mineral phase binaries, the following morphological parameters are determined for each phase of a given particle using standard image analysis routines: minimum, maximum, and average cross-sectional diameter; area; and external perimeter. Two correlation parameters are also determined for each mineral phase: an indication of whether the mineral grain is included, attached, or excluded relative to the coal matrix; and the amount of mineral perimeter in contact with the coal or mounting medium. In addition to this morphological and phase correlation data, compositional information is obtained by acquiring an energy-dispersive x-ray (EDX) spectrum from each mineral grain's center. Spectral regions-of-interest (ROI) are defined to measure the characteristic x-ray emission intensities of twelve common, mineral-forming, major and minor elements (Na, Mg, Al, Si, P, S, Cl, K, Ca, Ti, Fe, and Ba). Relative intensities are calculated by dividing the net counts for each element by the total ROI counts for all elements. Morphological, phase correlation, and compositional data are collected at three magnifications to provide the spatial resolution necessary to analyze particles ranging widely in size. These data are transferred on-line to a personal computer where it is tabulated and stored to disk for subsequent reduction, report generation, and archival. The acquired BSE images with the locations of EDX analysis are stored to tape.

5.4.2.3 Data Reduction and Reporting

A modified version of the PARTCHAR data reduction program (20) classifies the mineral compositional analyses based on elemental relative intensities, relative-intensity ratios, and stoichiometric criteria into one of 33 mineral/chemical and mineral association categories. Analyses that do not conform to any of the specified criteria are termed unclassified. The program allocates the classified particles according to average diameter into six intervals so that the size distribution of mineral/chemical phases can be determined. A report is generated that summarizes the results in a series of tables containing information on the number, area, and proportions of mineral/chemical phases in their respective size intervals and according to their association with the coal matrix (i.e., included, attached, or excluded). Mineral weight percentages are calculated assuming that particle area is proportional to particle volume (53) and mineral densities are constants.

5.4.3 Future Work

Development of the PBPSEM method is in its infancy and several refinements are required before it can be used routinely for characterizing coal mineralogy. The automatic threshold selection algorithm requires a bimodal gray-level histogram for segmenting the coal particles from mounting medium. This requirement is violated when the area imaged on a sample consists of only coal or mounting medium. Currently, the analysis is performed at low magnifications, generally less than 500 times, to prevent such an occurrence. This practice, however, results in rather poor spatial resolution, thereby limiting the method to analyzing relatively large particles, generally greater than about three microns in average cross-sectional diameter. Other procedures for automatic threshold selection are being investigated to negate this particle-size restriction. Another limitation of the method is the inability to distinguish and quantify mineral-mineral associations for agglomerated particles. This information is

extremely important when considering inorganic transformations that occur during combustion. The threshold selection algorithm currently employed cannot distinguish among various mineral species because of overlapping gray-level intensities. Additional development of the data reduction program is needed to present quantitative mineral-coal association results in formats appropriate for various applications, such as in the field of physical coal cleaning or ash modeling.

Work also needs to be done to optimize and validate the method. The PBPMSEM program is currently being tested. Data reduction is in progress; results of these preliminary tests will be discussed in the six-year final report, due in October 1992.

5.4.4 Conclusion

The PBPMSEM analysis method has been designed to provide detailed morphological and compositional information on the minerals in coal. Developmental efforts are in progress to optimize the method and assess its performance characteristics (e.g., limitations, repeatability). Work will also continue to extract and quantify the wealth of information provided by this method for various applications.

5.5 Mass Balancing of Inorganic Constituents in Coal

An algorithm to determine the distribution of organically associated inorganics was created using CCSEM, chemical fractionation, and XRF data. The CCSEM data need to be corrected with a ZAF-correction routine that adjusts the data based on atomic number (Z), absorption (A), and fluorescence (F), in order to better represent elemental weight percentages. The CCSEM data are characterized using the PARTCHAR program with a few modifications to allow for the differences between EDS and ZAF corrected numbers. The minerals are then grouped into mineral bins. A physical state and specific gravity are assumed from the mineral type, and the appropriate amount of each oxide is calculated. The major components as well as any impurities are all accumulated as equivalent oxides for each mineral since very few minerals are completely pure.

Data from the three techniques are used to divide the inorganics into soluble minerals, insoluble minerals, organically associated inorganics, and insoluble submicron minerals. The CCSEM data are normalized to the XRF data through a mass balance on silicon. Silicon is assumed to not be present as organically associated and a small amount (5%) is assumed to be submicron. The chemical fractionation and CCSEM data can then be combined on an equivalent oxide basis. The oxides removed during the chemical fractionation technique are either organically associated or soluble minerals. By subtracting out the soluble minerals found in the CCSEM technique, the amount of organically associated constituents can be determined. The amount of submicron inorganics that are insoluble can also be determined by mass balancing the remaining minerals with the XRF and chemical fractionation data. Any submicron minerals which are also soluble during the chemical fractionation technique will be included with the organically associated constituents.

The mass balance was run on the Kentucky #9, Eagle Butte, and Kentucky #9/Eagle Butte blend coals. The results for the three coals are shown in Figures 62, 63, and 64, respectively. These figures show the total

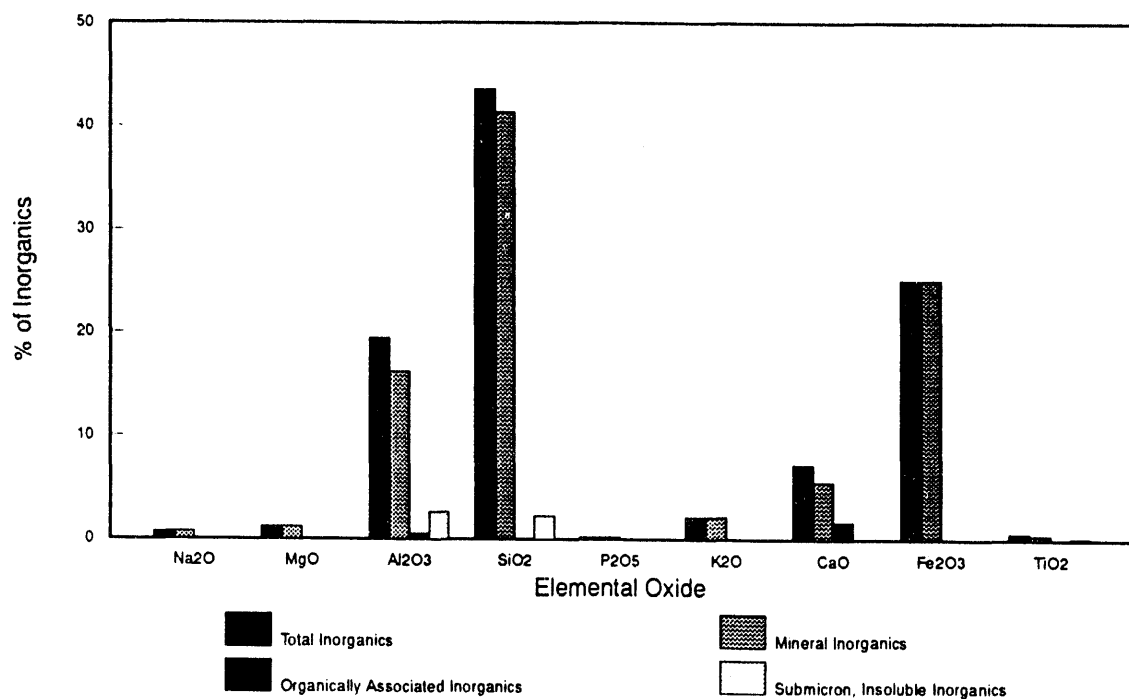


Figure 62. Mass balance results for Kentucky #9 coal.

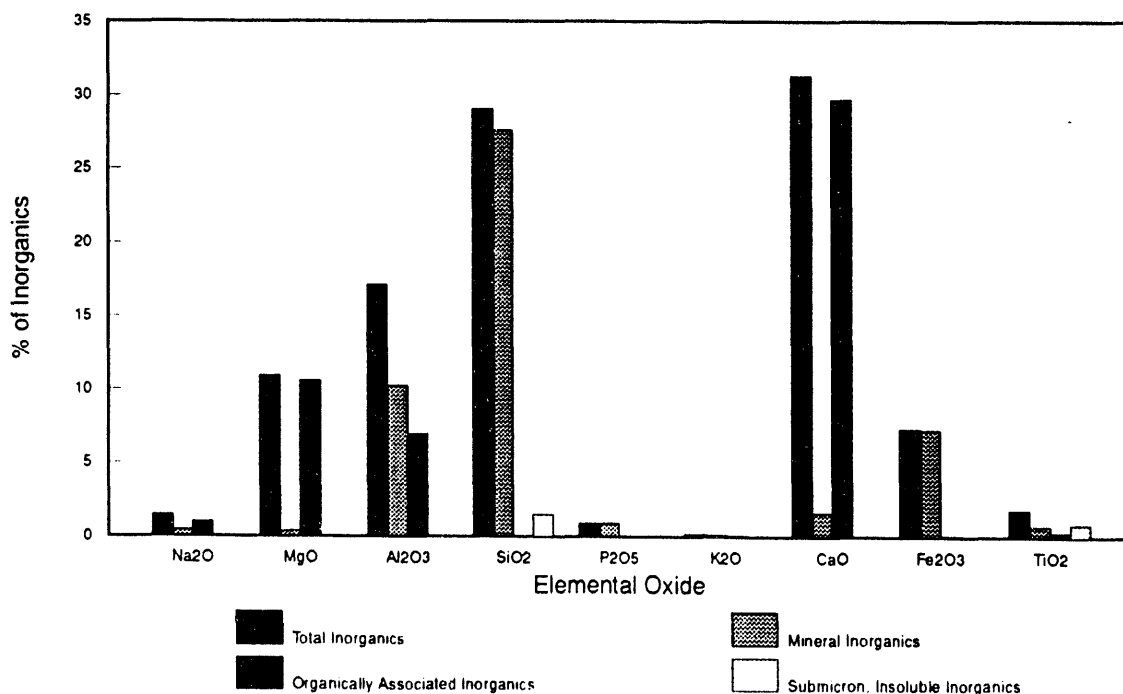


Figure 63. Mass balance results for Eagle Butte coal.

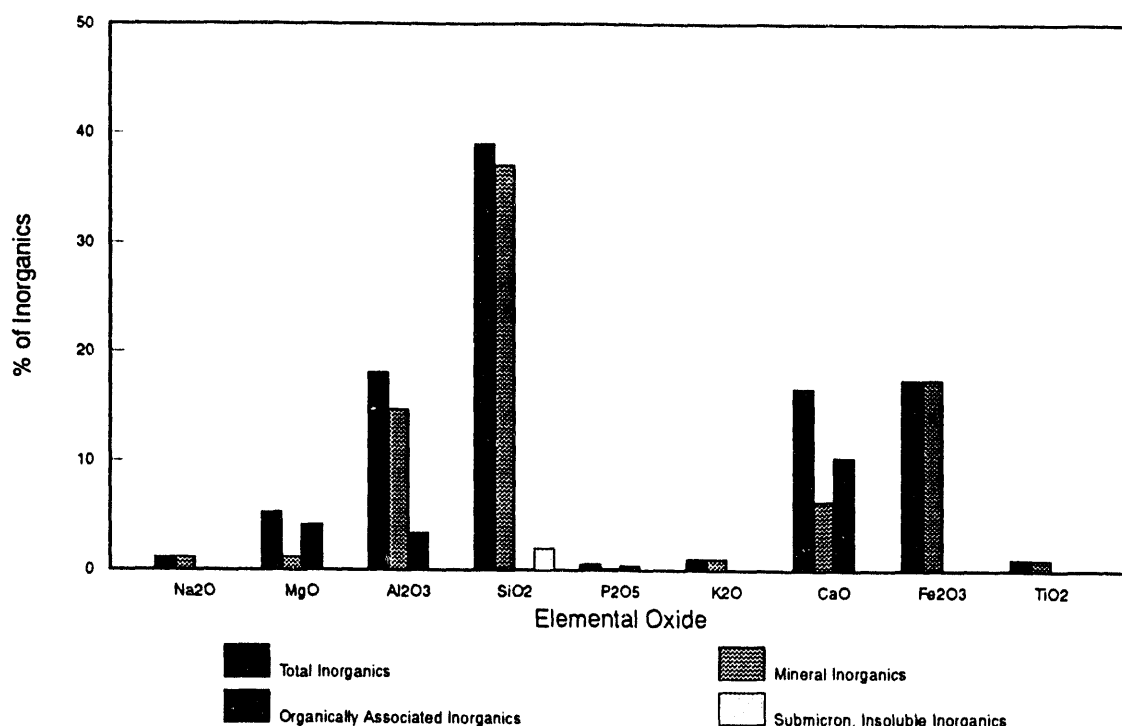


Figure 64. Mass balance results for Eagle Butte/Kentucky #9 blend coal.

inorganics, mineral inorganics, organically associated inorganics and submicron, insoluble inorganics. The Kentucky #9 shows very little organically associated constituents while the Eagle Butte has a large amount of organically associated calcium and magnesium. The blend lies between the two parent coals. As stated earlier all three coals have an assumed 5% submicron silicon. The submicron silicon is assumed to follow the general trend of the aluminum since they are often together as submicron clay particles. Only the Kentucky #9 coal shows a good correlation between the silicon and aluminum. An iterative balance between the silicon and aluminum would account for this better.

5.6 Analysis of Submicron Particles

5.6.1 Introduction

Scanning electron microscope analysis of coal and ash samples yields size and composition data on a particle-by-particle basis, information that is critical in predicting inorganic transformations during combustion. Through automated techniques, hundreds to thousands of individual particles can be chemically analyzed using energy-dispersive x-ray spectrometry and image processing. A minimum of operator effort is thus required to achieve a statistically significant characterization of the sample.

Electron microscope techniques developed at the EERC have previously been applied to mineral and ash particles with minimum diameters of 1 μm . However, individual-particle analysis is also important for particles with

diameter $<1 \mu\text{m}$. Submicron particles form during combustion from both organically-associated elements and from minerals in coal.

Most low-rank United States coals contain significant quantities of sodium, magnesium, and calcium, and lesser amounts of potassium, iron, and aluminum, all incorporated into the organic structure of the coal. These organically associated elements commonly vaporize during combustion. Sodium, magnesium, and potassium are particularly volatile and can condense homogeneously as submicron particles if the ratio of vapor phase alkali elements to ash surface area is large. These particles usually react with sulfur dioxide to form submicron sulfate particles by the time they reach the outlet of the boiler.

In contrast to the organically associated elements, mineral particles in coal undergo much less vaporization and condensation during combustion. The degree of vaporization depends on the composition of the local gas. If air is not vigorously mixed with the burning coal particles, reducing zones can exist in the flame. Within the reducing zones, silicon dioxide (SiO_2) in quartz and clays can be reduced to silicon monoxide (SiO), which is volatile. In cooler zones of the furnace, the SiO vapor will oxidize and condense as small SiO_2 particles in much the same way as the vaporized sodium species. However, in most pulverized coal boilers, mixing is rigorous enough that the formation of submicron SiO_2 particles is negligible.

Size reduction of mineral particles can also occur during rapid heating via decomposition or fragmentation. When rapidly heated, pyrite fractures and, upon partial oxidation, forms FeS fragments before melting at 1075°C (53). The extent to which this fragmentation contributes to the formation of submicron particles depends on the degree of mixing of fuel and air; pyrite produces more submicron particles in an oxidizing atmosphere. The carbonate minerals calcite (CaCO_3), siderite (FeCO_3), and ankerite ($\text{CaFe}[\text{CO}_3]_2$) also fragment upon decomposition to form submicron particles (53). In most cases the particle-size distribution of the ash produced during combustion is shifted toward smaller sizes than the size distribution of the coal minerals.

Once formed within the boiler, submicron particles are difficult to remove with particulate control devices. When emitted, these fine particles contribute far more to plume opacity per unit mass than do larger particles (54). The effect of the fine particles on plume opacity is maximized because their size distribution peaks near a diameter equal to the wavelength of visible light, the particle size with the greatest amount of scattering per unit mass (55,56). Understanding of the composition and formation of submicron particles is thus important in mitigating particulate emissions.

Submicron particles are difficult to analyze using automated techniques because their small size places them near the imaging and analytical detection limits of the conventional SEM. Using the recently-acquired ADEM (described above) and a new sample preparation method involving freeze-drying, individual ash particles with diameters as small as $0.1 \mu\text{m}$ can be analyzed automatically. The new technique is termed scanning electron microscopy with image analysis (SEM-IA), and is generally similar to CCSEM. The sample preparation method, SEM-IA technique, and some applications are described below.

5.6.2 Sample Preparation Method

A new sample preparation method was developed to enable automated SEM analysis of submicron particles. The method involves freeze-drying a small amount of dispersed particles onto a substrate of vitreous carbon. Vitreous carbon is used because its exceptionally smooth surface allows unambiguous identification of small particles. Freeze-drying maintains a uniform separation between particles.

Approximately 10 μg of particulate sample is suspended in 5 mL of purified propanol, to which a drop of dilute organic dispersant has been added. The propanol is first purified by filtration through a 0.05- μm pore polycarbonate filter. The suspension is vibrated ultrasonically for ten minutes to break up any loosely attached particles. Two to five drops of the suspension are placed on a clean piece of vitreous carbon measuring 15x10x3 mm. The sample assemblage is lowered into liquid nitrogen to freeze the particles and propanol into place. After the sample has cooled completely, it is removed from the liquid nitrogen and placed on top of a brass disk measuring approximately 25 mm in diameter and 12 mm in height. The brass disk was previously cooled in liquid nitrogen and serves as a heat sink to prevent overly rapid thawing of the sample. The sample and brass disk are positioned in the bell jar of a vacuum evaporator unit. Thawing under vacuum allows the propanol to evaporate gradually from the sample while preserving a constant spacing between particles. A vacuum of approximately 0.07 Pa is maintained during thawing.

The sample appears dry after approximately 30 minutes, but must remain under vacuum for an additional 60 to 90 minutes to allow its temperature to rise sufficiently to prevent condensation upon removal from the chamber. After removal, samples are coated with a 20-nm thick layer of vacuum-deposited carbon to improve conductivity. The freeze-dried dispersions are suitable for SEM-IA.

5.6.3 Scanning Electron Microscope Analysis of Submicron Particles

The Tracor-Northern ADEM is used for SEM-IA of the freeze-dried sample preparations. A low accelerating voltage (7 kV) is preferred to keep the excitation volume within the particles and to improve imaging. Secondary electron imaging (at 10,000x magnification) and derived binary images are used to locate and measure the size of each particle. The image analysis consists of acquiring 25 digital images of each field of view. The 25 images collected for each field are averaged to remove noise, creating a reference image for that field.

After an average image has been formed, individual ash particles are automatically sized, then analyzed for chemical composition using EDS. Spectra are acquired for 15 seconds at 300 pA. A relatively low-beam current is used to minimize sample damage. Spectra collected using these parameters generally contain sufficient x-ray counts to identify the elemental composition of most submicron particles. The use of a low accelerating voltage results in decreased detection efficiency for many metals, but this does not detract from the analysis of typical sulfate-bearing submicron particles.

A field of view contains approximately 20 individual ash particles. This relatively light particle loading is necessary to prevent electron beam overlap onto adjacent particles during EDS analysis. Each field of view must be manually selected by the operator. Currently, only approximately 200 particles per sample are analyzed because of the operator time required to select each field of view. As SEM-IA analyses become more routine, the number of particles analyzed per sample will increase.

Region-of-interest (ROI) integrated counts and particle-sizing information is saved in the ADEM computer as each field of view is completed. After each sample analysis is complete, the data files are transferred to the Tracor-Northern TN-8500 computer and reduced using the same routines applied to CCSEM data. The classification program PARTCHAR was modified to apply better to submicron particles by including more sulfate types and fewer metal-rich types. Modifications will continue in the future as more samples are characterized.

5.6.4 Tests of the SEM-IA Method

Visual inspection of the freeze-dried sample preparations in the ADEM shows that many individual submicron particles are present. In some instances several submicron particles are fused together to form irregularly shaped aggregates. Such aggregates are common in fly ash and probably form at elevated temperatures prior to emission (57,58). Alternatively, vapor-phase condensation may have occurred following aggregation, smoothing the spherule surfaces together through deposition of coatings. No attempt was made to break up these aggregates, as this would alter the size distribution of the original sample.

Several samples were analyzed to test the SEM-IA method. The analyses were designed to investigate any sampling bias and to compare SEM-IA with CCSEM results for identical samples. Fly ash samples produced from Eagle Butte coal and from a blend of Eagle Butte (70%) and Kentucky #9 (30%) coals were used. Each test is described separately below.

5.6.4.1 Test of Sampling Bias (Eagle Butte)

There was some concern that operator selection of fields of view could result in over representation of the smallest particles. However, large agglomerated groupings of particles are sometimes present in the sample preparation (probably the result of overloading the sample suspension), and so some operator discretion is necessary. A single freeze-dried preparation of Eagle Butte fly ash was analyzed twice using the SEM-IA method: first using fields of view selected because they contained relatively high proportions of submicron particles, then using randomly selected areas.

Size distributions of the two runs are shown in Figure 65. The two runs produced similar results, with both size distributions peaking at particle diameter of 0.4 μm . The run emphasizing submicron particles has a second peak at a particle diameter of 25 μm , indicating large agglomerates of particles were encountered in the area of the sample preparation used for this run. As mentioned above, these agglomerates are an artifact of the sample preparation procedure. It is not always possible to avoid these agglomerates when choosing fields of view. The agglomerates are easily identified by their

size distribution curve, which is distinctly separate from the curve representing the submicron particles (Figure 65) and can easily be removed from the data set after the analysis is completed.

The results of these two runs suggest that the true size distribution of the sample is accurately measured by the SEM-IA method. The peak at diameter 0.4 μm may indicate a uniformity of ash formation processes leading to a consistent particle size.

5.6.4.2 Comparison of SEM-IA and CCSEM Methods (Eagle Butte)

In order to directly compare SEM-IA and CCSEM results, the same freeze-dried dispersion of Eagle Butte fly ash was analyzed using both SEM-IA and CCSEM. In addition, a standard dispersion of the same ash sample was prepared and analyzed using CCSEM. Results are shown in Table 24. Particle compositions for the SEM-IA and CCSEM analyses are completely different, whereas the results for the two CCSEM runs are similar. Particles detected using SEM-IA are predominantly sulfate-, phosphate-, and chloride-rich, whereas those detected through CCSEM represent an assortment of minerals, mostly Ca-rich, including Ca aluminate, Ca-silicate, gypsum/Al-silicate, Ca-Al-silicate, and others. A minor amount of sulfate-rich particles are also present in the CCSEM data sets.

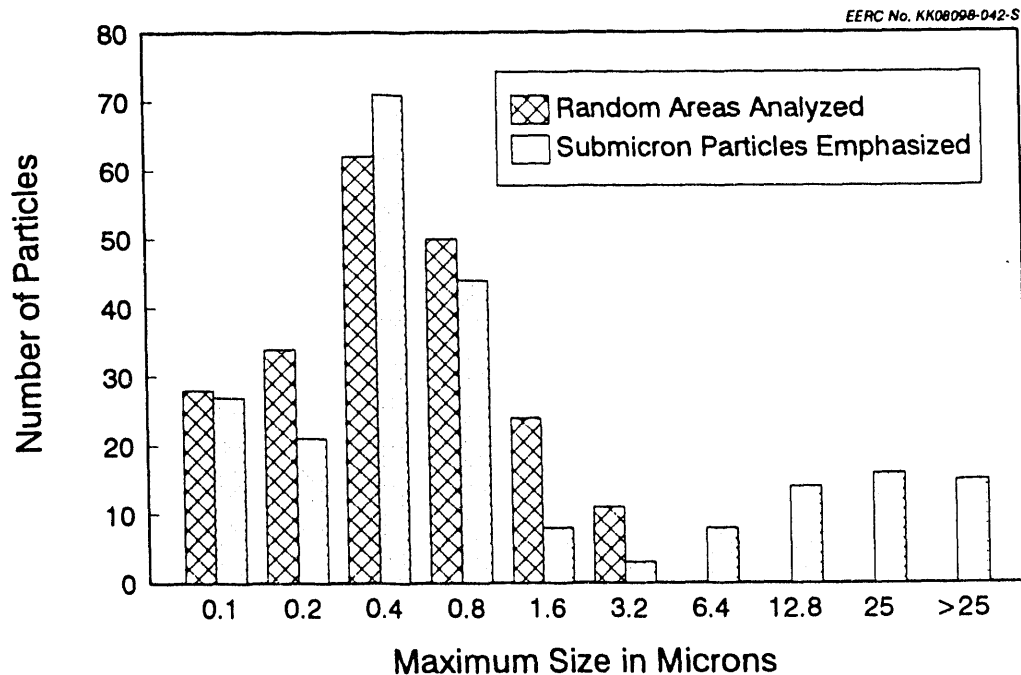


Figure 65. Size distributions for SEM-IA results for Eagle Butte parent ash, using a freeze-dried sample preparation.

The compositional variations between the SEM-IA and CCSEM data sets reflect the different size ranges represented by the two types of analyses. In the SEM-IA run, the maximum particle diameter in Table 24 was 1.6 μm . Large agglomerates, with diameters of 25 μm and greater, are sample preparation artifacts and were not included in the table. The CCSEM analyses include only particles with diameters $>1 \mu\text{m}$, and so most of the particles detected using SEM-IA would not be included in the CCSEM results.

It is less clear why the SEM-IA results do not include many particles with diameters in the low end of the CCSEM range, i.e., those with diameters of 2 to 10 μm . Apparently the fields of view selected for SEM-IA analysis contained few or no particles in this size range, in contrast to the areas used for CCSEM. Only a very small area of the sample was used to obtain data for 226 particles through SEM-IA. The CCSEM analysis of the same freeze-dried preparation included a much larger area (at lower magnification), yielding data for 453 particles. The CCSEM analysis of the standard dispersion

Table 24
Results of SEM-IA and CCSEM Analyses
Mineral weight percentages for Eagle Butte Fly Ash

Mineral	SEM-IA run (freeze-dry)	CCSEM run (freeze-dry)	CCSEM run (standard)
Quartz	0	3.8	6.5
Iron Oxide	0	1.6	0.2
Periclase	1.6	0	0
Alumina	0	0.3	0
Calcite	0	0.7	0.8
Dolomite	0	3.0	5.0
Kaolinite	0	1.5	0
Ca Al-Silicate	0	5.0	6.2
Na Al-Silicate	0	4.3	2.3
Mixed Al-Silicate	0	1.6	1.1
Ca-Silicate	0	6.5	2.6
Ca Aluminate	0	17.3	24.4
Sulfate-Rich	42.7	2.0	1.3
Phosphate-Rich	16.2	0	0
Chloride-Rich	11.4	0	0
Gypsum/Al-Silicate	0	5.8	2.8
Si-Rich	0	0.6	1.6
Ca-Rich	0	5.9	2.9
Ca-Si-Rich	0	2.2	2.6
Unknown	28.1	37.7	39.9
TOTALS	100.0	100.0	100.0

included 1013 particles. In the future, SEM-IA runs will be lengthened to make them more directly comparable with CCSEM analyses. The similarity between the results for the two CCSEM runs indicate that the freeze-dried preparation yields results similar to those of the standard dispersion.

The distinct compositional variation between the submicron size fraction (as measured using SEM-IA) and the supermicron fraction (measured using CCSEM) confirms that they are formed through different processes. Condensation of alkali vapors is evidently the primary mechanism for formation of submicron particles, while the mineral-rich content of the supermicron particles indicates they probably formed through decomposition and fragmentation.

5.6.4.3 Comparison of SEM-IA and CCSEM Methods (Eagle Butte/Kentucky #9 Blend)

The SEM-IA method was also evaluated by comparison with CCSEM results for ash from the Eagle Butte/Kentucky #9 70/30 blend. In this case, a freeze-dried dispersion was analyzed using SEM-IA, and a standard dispersion prepared from the same sample was analyzed using CCSEM (Table 25). As for the Eagle Butte ash samples discussed above, the results for the blend ash show distinct size-related compositional variations. The SEM-IA results, which include data for particles with a maximum diameter of 1.6 μm only, are dominated by sulfates, phosphates, and chlorides. No typical coal minerals were identified in the SEM-IA data set. Almost half of the particles identified using SEM-IA were classified as "unknown"; these may represent coated mineral particles or others of mixed composition.

The CCSEM data for the blend ash indicate a range of minerals. As for the Eagle Butte ash, the mass of the blend ash analyzed using CCSEM is concentrated in particles with diameters from 1 to 10 μm . The CCSEM results for the blend ash indicate more sulfate-rich particles and fewer Ca-bearing particles than the results for the Eagle Butte ash.

5.6.5 Conclusions

SEM-IA and CCSEM results for the Eagle Butte ash and the Eagle Butte/Kentucky #9 blend ash clearly indicate a size-related shift in composition, from mineral-rich particles in the supermicron fraction, to sulfate-, phosphate-, and chloride-rich particles in the submicron fraction. As more SEM-IA results are obtained, the particle classification scheme will be further refined to better identify coated and mixed particles currently grouped into the "unknown" category. Future SEM-IA analyses will include areas of the samples, in order to obtain data for a sufficient number of supermicron particles, for better comparison with CCSEM results. The results presented above show SEM-IA to be a promising technique for characterization of submicron particles. The unique compositions of particles in the submicron size fraction suggest that individual-particle analysis of these smallest particles is essential to achieving an overall understanding of the transformations occurring during combustion.

Table 25

Results of SEM-IA and CCSEM Analyses
Mineral Weight Percentages for Eagle Butte/Kentucky #9 Blend Ash

Mineral	SEM-IA (freeze-dry)	CCSEM (standard)
Quartz	0	6.5
Iron oxide	0	0.5
Rutile	0	0.1
Alumina	0	0.1
Calcite	0	1.4
Ankerite	0	0.2
Kaolinite	0	6.3
Montmorillonite	0	1.8
K Al-silicate	0	0.5
Fe Al-silicate	0	3.9
Ca Al-silicate	0	9.2
Na Al-silicate	0	9.7
Aluminosilicate	0	0.1
Mixed Al-silicate	0	2.4
Ca silicate	0	1.9
Ca aluminate	0	1.4
Sulfate-rich	24.5	17.7
Phosphate-rich	13.4	0
Chloride-rich	14.7	0
Gypsum/Al-silicate	0	3.0
Si-rich	0	3.0
Ca-rich	0	0.1
Ca-Si-rich	0	0.6
Unknown	47.4	29.4
Totals	100.0	100.0

6.0 CONCLUSIONS

6.1 Task 1

Work on ASHPERT has included the development of algorithms for predicting ash particle-size distribution (PSD) and mineral frequency distribution (MFD) from the corresponding parent coals' PSDs and MFD. The database for this expert system currently contains the proximate/ultimate, XRF, chemical fractionation, and CCSEM data for 45 samples. In addition, the database also contains the sample's name, rank, location, biography, and ownership category. Routines to manage and analyze the database were also developed. To date, four different topologies and two different transformation models have been implemented and tested. The MARS topology with the linear transformation model emerges as the best "rule" for endowing

ASHPERT with the requisite expertise. The MARS topology "predicted" values are, on average, in error by about 8%. It is interesting to observe that the entire ASHPERT database of over 15 megabytes has been defined by a linear operator (a matrix in this case) requiring only about 5 kilobytes.

As to future directions for ASHPERT, a rigorous justification of the continuity hypothesis needs to be undertaken. Additional transformation models, especially nonlinear ones, need to be tested, since this may permit better correlations to be established with a smaller basis set than the currently used set of mineral types. The replacement of the linear operator by a neural network is very viable and would be a significant improvement. Additional analyses of the database need to be performed to extract possible parameters for the deterministic and stochastic classes of models. Such models need to be incorporated as part of ASHPERT's knowledge base, which will then allow ASHPERT to approximate fly ash distributions at various "stages" or locations within a combustor. Finally, additional work on the theoretical aspects of particle size and composition distribution (PSCD) evolution is also needed to improve our understanding of the physical and chemical processes involved in this complex transformation.

A mechanistic model for fly ash composition and size prediction was also devised. This model, ATRAN1, employs stochastic principles of mathematical random-combining of coal inorganic constituents to form the predicted fly ash. An algorithm has been formulated so that organically bound inorganic constituents are included in the program. Three coals were tested using the predictive model: Eagle Butte, Kentucky #9, and a blend of Kentucky #9 (30%) and Eagle Butte (70%). Preliminary results revealed that the Eagle Butte contained a larger amount of nucleated submicron particles due to the large amount of organically associated constituents present in the coal. Experimental fly ash produced using particle residence times and temperatures associated with fouling conditions in a boiler have not yet been generated on the coals in order to compare experimental and predicted fly ash composition and size. However, experimental fly ash was generated under slagging conditions (shorter particle residence times than fouling conditions) for the blend. The CCSEM mineral/phase composition of the experimental blend fly ash compared fairly well with that of the predicted blend composition, the only variances being with the complex aluminosilicates. Particle-size distributions also compared fairly well between the experimental and predicted blends.

6.2 Task 2

The tests performed on synthetic coal model mixtures were completed. Reaction kinetics determinations revealed that the state of Ca (organic or inorganic) in the Ca-Si-S system had a significant effect on the combustion of the synthetic chars. Detailed characterization of the Ca(min.)-S-Si system was performed to elucidate interactions between calcium, silica, and sulfur. Extensive surface condensation of CaO and calcium sulfate was observed at gas temperatures of 1300°C or lower. The formation of calcium silicate was most extensive at 1500°C. Fly ash particle sizes were larger at 900° and 1100°C than at 1300° and 1500°C, possibly because of more sticky calcium sulfate-silicate glue available at the lower temperatures. Char and calcite fragmentation was evident when combusting the Ca(min.)-Si-S mixture at 1500°C. The Fe(min.)-Al-Si system loses nearly all the sulfur from the pyrite at 900°C, leaving kaolinite and iron oxide. The system shows only a small degree

of interaction between the kaolinite and iron until 1500°C, when an increased amount of iron aluminosilicate components form.

A blend of 70% Wyoming Eagle Butte low-sulfur (<1% mf) subbituminous coal and 30% Kentucky #9 high-sulfur (4% mf) bituminous coal was analyzed using CCSEM. Experimental fly ash was generated in the DTF under slagging conditions, using a gas temperature of 1500°C and residence time of about 2.5 seconds. Ash was also produced under fouling conditions, using an extended residence time and lower temperatures. The fly ash was analyzed using SEMPC and CCSEM. Coal analyses revealed that the blending operation was quite successful as the physical and chemical components are nearly weighted averages of the components in the parent coals. The fly ash revealed very little interaction between the mineral components of the two different coals. Viscosity distributions of liquid phases in the fly ash under slagging conditions, for the experimental ash and a weighted average of the parent fly ashes, were similar. Iron-rich particles derived from the pyrite in the Kentucky #9 coal experienced only limited interaction with aluminosilicates, most of which had sources in the Kentucky #9.

6.3 Task 3

A round-robin CCSEM analysis has been initiated which involves seven laboratories, including UNDEERC, Ames Laboratory-Iowa State University, Sandia National Laboratory, the University of Kentucky, the R.J. Lee Group, the Netherlands Energy Research Center, and CSIRO of Australia. Three Argonne National Laboratory premium coals including Illinois #6, Pittsburgh #8, and Wyodak were prepared by CSIRO for potential analysis. Information was gathered from each of the participating laboratories regarding their CCSEM system and used to prepare a standard format for how the participants should configure their SEM system to analyze the coals. The results of the preliminary round-robin testing will be used to design further testing and refinement of the CCSEM technique, possibly leading to eventual certification of the method by an appropriate professional society.

A correction for improving the accuracy of CCSEM elemental compositions was devised. This procedure involves the extraction of k-ratios during acquisition of CCSEM data, followed by correction of these k-ratios for atomic number (Z), absorption (A), and fluorescence (F) effects. This ZAF correction results in more accurate quantitative chemistries of individual fly ash particles or minerals. Five ash samples and three coals were analyzed to test the CCSEM-ZAF technique. Bulk composition of these ashes and coals were calculated from the CCSEM-ZAF data and compared to bulk compositions derived from XRF and SEMPC analyses. Results indicate a reasonable correspondence between the techniques, with the exception of elements commonly concentrated in the organic matrix and/or the submicron particulate size fraction.

A semiautomated PBPSEM analysis technique was devised and refined into a fully automated technique. This new technique uses advanced image analysis along with the standard CCSEM procedure to give the size and composition of coal minerals on an individual coal-particle basis. This technique greatly enhances ash formation and deposition models by providing much more comprehensive coal input data. The major operating parameter affecting the sizing and location of particles is the determination of the difference between coal and minerals in the gray-level histogram. The method now used to determine this difference works well for completely homogeneous systems.

Present efforts are focused on determining the reproducibility of gray-level histograms in heterogeneous coal systems and developing ways of improving the distinction between the different components in the system. Samples are currently being tested to determine the accuracy of the PBPSEM technique.

A method has been devised to mass balance organically and mineralogically associated inorganics in coal so that their sum equals the total ash content of the coal. An algorithm to determine the distribution of organically associated inorganics was created using computer controlled scanning electron microscopy (CCSEM), chemical fractionation, and x-ray fluorescence (XRF) data. Data from the three techniques are used to divide the inorganics into soluble minerals, insoluble minerals, organically associated inorganics, and insoluble submicron minerals. The mass balancing technique was tested on the Kentucky #9, Eagle Butte, and Kentucky #9/Eagle Butte blend coals. Kentucky #9 coal contained very little organically associated constituents, whereas the Eagle Butte coal had a large amount of organically associated calcium and magnesium. The organically bound content for the Kentucky #9/Eagle Butte blend was intermediate between the two parent coals.

A new method for automated analysis of individual submicron particles has been developed. Scanning electron microscopy with image analysis (SEM-IA) is similar to the CCSEM method for larger particles, but uses the Tracor-Northern ADEM to enable analysis of particles as small as 0.1 μm in diameter. Preliminary results show the submicron fractions of ash samples to have an entirely different composition from that of the larger particles. The submicron size fraction typically contains sulfates, phosphates, chlorides, and mixed particles, compared with the aluminosilicates and Ca-rich particles found in the supermicron fractions. The distinct compositions of the two size fractions confirm that they form through different processes, probably primarily fragmentation and coalescence for the supermicron particles, and vaporization and condensation for the submicron particles.

7.0 REFERENCES

1. Zygarlicke, C.J.; McColler, D.P.; Toman, D.L.; Erickson, T.A.; Ramanathan, M.; Folkedahl, B.S. "Combustion Inorganic Transformations," Semiannual Technical Progress Report for the Period July 1, 1991 - December 31, 1991. USDCE Cooperative Agreement No. DE-FC21-86MC10637, 1992.
2. Benson, S.A.; Holm, P.L. "Comparison of Inorganic Constituents in Three Low-Rank Coals," *Ind. Eng. Chem. Prod. Res. Dev.* 1985, 24, 145.
3. Kalmanovitch, D.P.; Montgomery, G.G.; Steadman, E.N. "Computer-Controlled Scanning Electron Microscope Characterization of Coal Ash Deposits," ASME Paper Number 87-JPGC-FACT-4, 1987.
4. Dunn-Rankin, D. "Kinetic Model for Simulating the Evolution of Particle Size Distribution During Char Combustion," *Combust. Sci. and Tech.* 1988, 58, 297-314.

5. Huang, J.; Edwards, B.F.; Levine, A.D. "General Solutions and Scaling Violations for Fragmentation With Mass Loss," Department of Physics, West Virginia University, 1991, preprint.
6. Baxter, L.L.; Abbot, M.F.; Douglas, R.E. "Dependence of Elemental Ash Deposit Composition on Coal Ash Chemistry and Combustor Environment," 1991, preprint.
7. Cai, M.; Edwards, B.F.; Han, H. "Exact and Asymptotic Scaling Solutions for Fragmentation with Mass Loss," *Phys. Rev.* **1991**, *A* (43), 656-662.
8. Beer, J.M.; Sarofim, A.F.; Barta, L.E. "From Coal Mineral properties to Fly Ash Deposition Tendencies: A Modelling Route," *J. Inst. Energy* **1992**, *65*, 55-62.
9. Kerstein, A. R.; Edwards, B.F. "Percolation Model for Simulation of Char Oxidation and Fragmentation with Time-Histories," *Chem. Eng. Sci.* **1987**, *42*, 1629-1634.
10. Edwards, B. F.; Ghosal, G.K. "Model of Ash Size Distributions from Coal Char Oxidation," Department of Physics, West Virginia University, 1991, preprint.
11. Ullman, J.D. "Principles of Database and Knowledge-Based Systems, Vol. I: Classical Database Systems," Comp. Sci. Press: Maryland, 1988.
12. Goldstein, J. I.; Newbury, D.E.; Echlin, P.; Joy, D.C.; Fiori, C; Lifshin, E. "Scanning Electron Microscopy and X-Ray Microanalysis," Plenum Press: ew York, 1981.
13. Dinger, D. R. "New Stereological Method for Obtaining 3-Dimensional Grain Size Distributions and Shape Factors from Planar Sections: Application to Characterization of Mineral Matter in Coal," Ph.D. Thesis, Pennsylvania State University, 1975.
14. DeHoff, R. T.; Rhines, F.N. "Quantitative Microscopy," McGraw-Hill: ew York, 1968.
15. Ramanathan, M. "Particle Size and Composition Distribution in Coal Combustion Systems: Phenomenology and Expertise," *In Proceedings of the Expert System Applications for the Electric Power Industry*, Boston, MA, September 9-11, 1991.
16. Senior, C.L. "Submicron Aerosol Production During Combustion of Pulverized Coal," Ph.D. Thesis, California Institute of Technology, 1984.
17. Erickson, T.A. "The Fate of Flame Volatilized Sodium during the Combustion of Pulverized Coal in Reaction with Silica and Sulfur (Studied with the Aid of a Synthetic Coal)," Masters Thesis, University of North Dakota, 1990.
18. Ludlow, D.K.; Erickson, T.A.; Benson, S.A. *Energy and Fuels* **1991**, *5*, 539.

19. Zygarlicke, C.J.; Toman, D.L.; Erickson, R.A.; Ramanathan, M.; Folkedahl, B.C. "Combustion Inorganic Transformations," Final Technical Progress Report for the Period July 1, 1990 - June 30, 1991, USDOE Contract No. DE-FC21-86MC10637, University of North Dakota Energy and Environmental Research Center, Grand Forks, ND, 1991.
20. Zygarlicke, C.J.; Steadman, E.N. "Advanced SEM Techniques to Characterize Coal Minerals," *Scanning Microsc. Int.* 1990, 4 (3), 579.
21. McCollor, D.P.; Jones, M.L.; Benson, S.A.; Young, B.C. 22nd International Symposium on Combustion, The Combustion Institute, Pittsburgh, 1988, p 59.
22. Kalmanovitch, D.P.; Frank, M. "An Effective Model of Viscosity for Ash Deposition Phenomena," Presented at the Conference on Mineral Matter and Ash Deposition from Coal, The Engineering Foundation, Santa Barbara, CA, February 21-26, 1988.
23. Vorres, K.S. *Users Handbook for the Argonne Premium Coal Sample Program*; Argonne National Laboratory, 1989, 64 p.
24. Vorres, K.S. "The Argonne Premium Coal Sample Program," *Energy & Fuels* 1990, 4 (5), 420-426.
25. Lee, R.J.; Kelly, J.F. "Overview of SEM-Based Automated Image Analysis," *Scanning Electron Microscopy* 1980, 1, 303-310.
26. Huggins, F.E.; Kosmack, D.A.; Huffman, G.P.; Lee, R.J. "Coal Mineralogies by SEM Automatic Image Analysis," *Scanning Electron Microscopy* 1980, 1, 531-540.
27. Huggins, F.E.; Huffman, G.P.; Lee, R.J. "Scanning Electron Microscope-Based Automated Image Analysis (SEM-AIA) and Mössbauer Spectroscopy: Quantitative Characterization of Coal Minerals," In *Coal and Coal Products: Analytical Characterization Techniques*; Fuller, E.L. Jr., Ed.; American Chemical Society Symposium Series 205, 1982, Chapter 12, p. 239-258.
28. Straszheim, W.E.; Markuszewski, R. "Automated Image Analysis of Minerals and Their Association with Organic Components in Bituminous Coals," *Energy & Fuels* 1990, 4 (6), 748-754.
29. Straszheim, W.E.; Markuszewski, R. "Engineering Insights from Automated Image Analysis of Mineral Matter in Coal," In *Mineral Matter and Ash Deposition from Coal*; Bryers, R.W.; Vorres, K.S., Eds.; Engineering Foundation: New York, 1990, pp 53-61.
30. Straszheim, W.E.; Markuszewski, R. "Automated Image Analysis of the Association of Ash-Forming Mineral Matter with Coal Particles," *Prepr. Pap.--Am. Chem. Soc., Div. Fuel Chem.* 1991, 36 (1), 216-222.

31. Straszheim, W.E.; Yousling, J.G.; Younkin, K.A.; Markuszewski, R. "Mineralogical Characterization of Lower-Rank Coals by SEM-Based Automated Image Analysis and Energy Dispersive X-Ray Spectrometry," *Fuel* 1988, 67, 1042-1047.
32. Zygarlicke, C.J.; Steadman, E.N.; Benson, S.A. "Studies of Transformations of Inorganic Constituents in a Texas Lignite During Combustion," *Prog. Energy Combust. Sci.* 1990, 16, 195-204.
33. Jones, M.L.; Kalmanovitch, D.P.; Steadman, E.N.; Zygarlicke, C.J.; Benson, S.A. "Application of SEM Techniques to the Characterization of Coal and Coal Ash Products," In *Advances in Coal Spectroscopy*; Meuzelaar, M.L.C., Ed.; Plenum Publishing Corp.: New York, 1992; Chapter 1, pp 1-27.
34. Casuccio, G.S.; Gruelich, F.A.; Hamburg, G.; Huggins, F.E.; Nissen, D.A.; Vleeskens, J.M. "Coal Mineral Analysis: A Check on Interlaboratory Agreement," *Scanning Microscopy* 1990, 4 (2), 227-236.
35. Vleeskens, J.M.; Hamburg, G. "Coal Minerals Analysis 'Round Robin,' Data Compilation," *Stichting Energieonderzoek Centrum Nederland*, ECN-89-154 (December 1987, updated October 1989), unpublished ECN internal report, 25 p.
36. Birk, D. "Coal Minerals: Quantitative and Descriptive SEM-EDX Analysis," *Journal of Coal Quality* 1989, 8 (2), 55-62.
37. Hamburg, G. "Description of the Tracor Northern Energy Dispersive System as Applied to Coal Minerals Analysis," *Technology in Review* 1984, 2 (1), 7-10.
38. Doughten, M.W.; Gillison, J.R. "Determination of Selected Elements in Whole Coal and in Coal Ash from the Eight Argonne Premium Coal Samples by Atomic Absorption Spectrometry, Atomic Emission Spectrometry, and Ion-Selective Electrode," *Energy & Fuels* 1990, 4 (5), 426-430.
39. Palmer, C.A. "Determination of Twenty-Nine Elements in Eight Argonne Premium Coal Samples by Instrumental Neutron Activation Analysis," *Energy & Fuels* 1990, 4 (5), 436-439.
40. Evans, J.R.; Sellers, G.A.; Johnson, R.G.; Vivit, D.V.; Kent, J. "Analysis of Eight Argonne Premium Coal Samples by X-Ray Fluorescence Spectrometry," *Energy & Fuels* 1990, 4 (5), 440-442.
41. Wertz, D.L. "X-Ray Analysis of the Argonne Premium Coals: 1. Use of Absorption/Diffraction Methods," *Energy & Fuels* 1990, 4 (5), 442-447.
42. American Society for Testing and Materials. "Practice for Conducting an Interlaboratory Study to Determine the Precision of Test Methods (E691)," *Annual Book of ASTM Standards* 1992, 14.02.
43. Association of Official Analytical Chemists. "AOAC Guidelines for Collaborative Study Procedure to Validate Characteristics of a Method of Analysis," *Journal of the Association of Official Analytical Chemists* 1988, 71, 161.

44. Horwitz, W. "Protocol for the Design, Conduct, and Interpretation of Collaborative Studies," *Pure and Applied Chemistry* 1988, 60 (6), 855-864.
45. Galbreath, K.C., Brekke, D.W., and Folkedahl, B.C. "Automated Analytical Scanning Electron Microscopy and Image Analysis Methods for Characterizing the Inorganic Phases in Coal and Coal Combustion Products," *ACS Fuel Chem. Division Preprints* 1992, 37 (in press).
46. Straszheim, W.E.; Younkin, K.A.; Greer, R.T.; Markuszewski, R. "Mounting Materials for SEM-Based Automated Image Analysis of Coals," *Scanning Microscopy* 1988, 2 (3), 1257-1264.
47. American Society for Testing and Materials (ASTM). "Standard Practice for Preparing Coal Samples for Microscopical Analysis by Reflected Light (D2797)," *Annual Book of ASTM Standards* 1991, 5.05, 308-311.
48. Wagner, A.M.; Pekowsky, B.C. "Locked and Liberated Analysis," *Tracor Northern Advanced Imaging Applications* 1989, Tracor Northern, Middleton, Wisconsin, p 4.
49. Lloyd, G.E. "Atomic Number and Crystallographic Contrast Images with the SEM: A Review of Backscattered Electron Techniques," *Mineralogical Magazine* 1987, 51, 3-19.
50. Twogood, R.E.; Sommer, F.G. "Digital Image Processing," *IEEE Transactions on Nuclear Science* 1982, NS-29 (3), 1076-1086.
51. Weszka, J.S. "A Survey of Threshold Selection Techniques," *Computer Graphics and Image Processing* 1978, 7, 259-265.
52. Kohler, R. "A Segmentation System Based on Thresholding," *Computer Graphics and Image Processing* 1981, 15, 319-338.
53. Raask, E. "Mineral Impurities in Coal Combustion," New York: Hemisphere Publishing Corp., 1984.
54. Balfour, D.A.; Meserole, F.M.; Defries, T. "Utility Stack Opacity Troubleshooting Guidelines," Final report, EPRI Research Project No. 2250-3, 1991.
55. Mie, G. "Beitrage zur Optik truber Medien speziell kolloidaler Metallosungen," *Ann. Phys.* 1908, 25, 377-445.
56. Bohren, C.F.; Huffman, D.R. "Absorption and Scattering of Light by Small Particles," New York: John Wiley & Sons: 1983, 530 p.
57. Hazrati, A.; Schrodtt, J.T. "Microcharacterization of Micron/Submicron Fly Ash from a Pulverized-Dry-Coal-Burning Power Plant," *Surf. Interface Anal.* 1988, 13, 142-148.
58. Kaufherr, N.; Lichtman, D. "Comparison of Micron and Submicron Fly Ash Particles Using Scanning Electron Microscopy and X-Ray Elemental Analysis," *Environ. Sci. Technol.* 1984, 18 (7), 544-547.

APPENDIX A

SUMMARY OF ORGANICALLY BOUND CONSTITUENTS IN PARENT COALS AND BLEND

**SUMMARY OF ORGANICALLY BOUND CONSTITUENTS IN PARENT COALS AND BLEND
(wt% Coal Basis)**

Eagle Butte

	Initial (ppm)	Removed by H ₂ O (%)	Removed by NH ₄ OAc (%)	Removed by HCl (%)	Remaining (%)
Silicon	7,325	0	0	0	100
Aluminum	4,889	0	11	35	54
Iron	2,770	2	0	68	30
Titanium	580	0	17	0	83
Phosphorus	215	0	34	57	9
Calcium	12,084	0	70	30	0
Magnesium	3,552	0	85	12	3
Sodium	573	16	78	2	4
Potassium	85	0	41	0	59

Kentucky #9

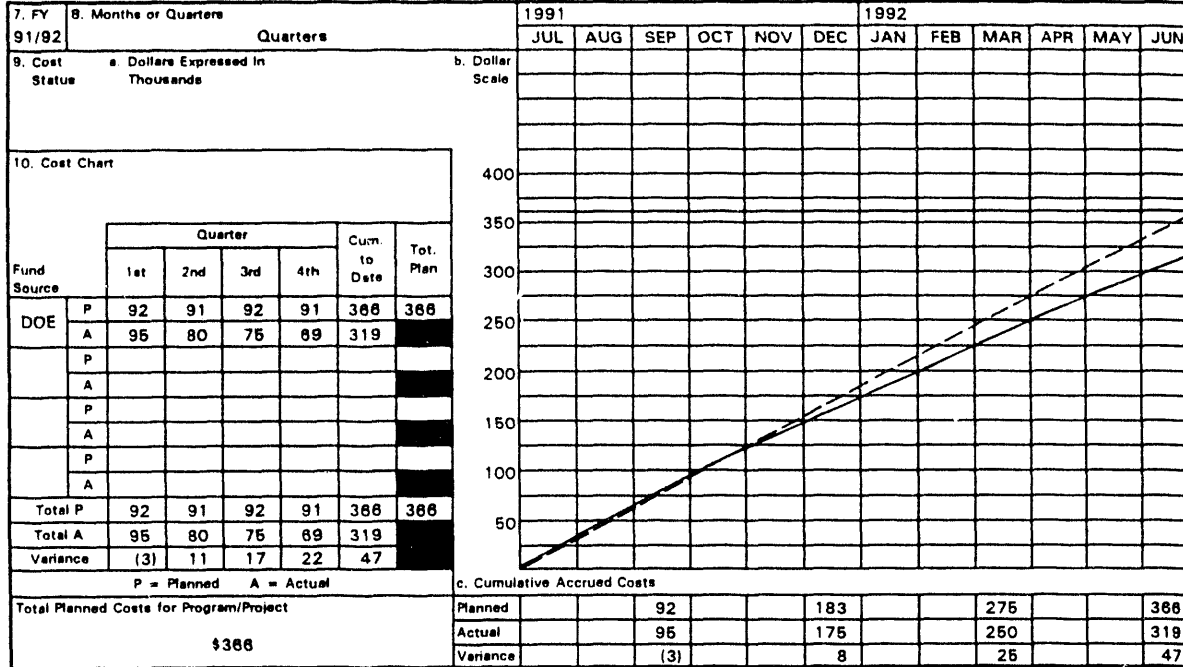
	Initial (ppm)	Removed by H ₂ O (%)	Removed by NH ₄ OAc (%)	Removed by HCl (%)	Remaining (%)
Silicon	28,526	0	0	0	100
Aluminum	14,401	0	0	3	97
Iron	24,625	14	0	6	80
Titanium	538	0	0	0	100
Phosphorus	129	6	51	43	0
Calcium	7,227	34	59	1	6
Magnesium	990	3	16	14	68
Sodium	739	30	33	2	35
Potassium	2,503	2	6	4	88

70/30 Blend

	Initial (ppm)	Removed by H ₂ O (%)	Removed by NH ₄ OAc (%)	Removed by HCl (%)	Remaining (%)
Silicon	16,109	0	0	0	100
Aluminum	8,416	0	0	22	78
Iron	10,753	20	0	20	60
Titanium	561	0	0	0	100
Phosphorus	227	0	35	60	6
Calcium	10,481	5	66	26	3
Magnesium	2,819	8	74	9	9
Sodium	747	47	33	3	16
Potassium	711	0	0	0	100

U.S. DEPARTMENT OF ENERGY
FEDERAL ASSISTANCE MANAGEMENT SUMMARY REPORT

1. Program/Project Identification No. DE-FC21-86MC10637	2. Program/Project Title Combustion Inorganic Transformations (3.2)	3. Reporting Period 4-1-92 through 6-30-92
4. Name and Address Energy and Environmental Research Center University of North Dakota Box 8213, University Station, Grand Forks, ND 58202 (701) 777-5000		5. Program/Project Start Date 4-1-86
		6. Completion Date 9-30-92



11. Major Milestone Status	Units Planned	
	Units Complete	
1. Fly Ash Particle-Size and Composition Prediction	P	a v b v c v d e v f v g A
	C	
	P	
	C	
2. Laboratory-Scale Combustion Testing	P	a v b v c d v e v f v g A
	C	
	P	
	C	
3. Analytical Methods Development	P	a v d v f v c v g v e v b v h A
	C	
	P	
	C	
4. Collaborative Research	P	a A
	C	
	P	
	C	
	P	
	C	
	P	
	C	
	P	
	C	
	P	
	C	
	P	
	C	

12. Remarks
Due to the EERC fiscal year end, the June books do not close until July 25, 1992. Costs posted through July 8 have been included.

13. Signature of Recipient and Date
[Signature]

14. Signature of DOE Reviewing Representative and Date

U. S. DEPARTMENT OF ENERGY
FEDERAL ASSISTANCE MANAGEMENT SUMMARY REPORT

1. Program/Project Identification No. DE-FC21-86MC10637		2. Program/Project Title Combustion Inorganic Transformations (3.2)		3. Reporting Period 4-1-92 through 6-30-92	
4. Name and Address Energy and Environmental Research Center University of North Dakota Box 8213, University Station Grand Forks, ND 58202 (701) 777-5000				5. Program/Project Start Date 4-1-86	
				6. Completion Date 9-30-92	
Milestone ID. No.	Description	Planned Completion Date	Actual Completion Date	Comments	
Task 1	Fly Ash Particle-Size and Composition Prediction:				
1.a	Production of experimental fly ash for Eagle Butte, Beulah, and Eagle Butte/Kentucky #9 blend coals.	7-31-91	7-31-91		
1.b	Addition of coal mineral and corresponding drop-tube furnace fly ash data from a low-rank and a high-rank coal to the ASHPERT model.	10-31-91	10-31-91		
1.c	Testing of stochastic model on Eagle Butte, Beulah, and Eagle Butte/Kentucky #9 blend. Stochastic model refinement and assessment of strengths and weaknesses.	11-15-91	11-15-91		
1.d	Refinement of the ASHPERT model to include organically bound inorganics in the prediction process.	11-30-91	11-30-91		
1.e	Expansion of the ASHPERT knowledge base to 40 coals and fly ashes.	3-31-92	3-31-92		
1.f	Testing of the ASHPERT model on four coals.	5-31-92			
1.g	Compilation of a document explaining the contents of the ASHPERT data base and the expert-system process.	6-15-92			
Task 2	Laboratory-Scale Combustion Testing:				
2.a	Formulate a synthetic coal/char model mixture with included inorganics consisting of pyrite and aluminosilicate.	8-31-91	8-31-91		
2.b	Characterize char and fly ash from the Eagle Butte/Kentucky #9 blend and evaluate mineral coalescence and fragmentation phenomena.	11-15-91	11-15-91		
2.c	Determination of char reactivity by calculating reaction kinetics during the combustion of Eagle Butte, Beulah, and Eagle Butte/Kentucky #9 blend coals.	12-31-91	12-31-91		
2.d	Combustion testing of the pyrite-aluminosilicate model mixture to note inorganic transformations and pyrite fragmentation.	1-31-92	12-31-91		
2.e	Mineral transformations under fuel-rich conditions in the drop-tube furnace.	3-15-92	3-15-92		

U.S. DEPARTMENT OF ENERGY
FEDERAL ASSISTANCE MANAGEMENT SUMMARY REPORT

1. Program/Project Identification No. DE-FC21-86MC10637		2. Program/Project Title Combustion Inorganic Transformations (3.2)		3. Reporting Period 4-1-92 through 8-30-92	
4. Name and Address Energy and Environmental Research Center University of North Dakota Box 8213, University Station Grand Forks, ND 58202 (701) 777-5000				5. Program/Project Start Date 4-1-86	
				6. Completion Date 9-30-92	
Milestone ID. No.	Description	Planned Completion Date	Actual Completion Date	Comments	
2.f	Consideration activity report for conducting future drop-tube furnace studies in ash deposition.	5-31-92			
2.g	Comparison of drop-tube furnace fly ash properties with those generated at the pilot or full scale.	6-15-92			
Task 3	Analytical Methods Development:				
3.a	The ZAF correction procedure for CCSEM chemistries will be tested, and the computer program for its use will be made user friendly.	10-31-91	10-31-91		
3.b	Results of the first round of samples being analyzed by the round-robin participants will be compiled.	6-15-92			
3.c	The particle-by-particle SEM (PBPSEM) method for coal analysis will be completed.	4-15-92			
3.d	Develop SEM technique to analyze coal minerals or ash particles that are less than 5µm.	1-31-92	1-31-92		
3.e	Round-robin results will be reported, and suggestions will be made for standardization of the CCSEM technique.	2-29-92			
3.f	Investigation of mass-balancing inorganics in low-rank coal using chemical fractionation and CCSEM.	3-31-92	3-31-92		
3.g	Testing of the PBPSEM method will be performed on previously analyzed coals.	5-31-92			
3.h	Meeting(s) will be held with ASTM officials for guidance in the ASTM standardization process.	6-30-92			
Task 4	Collaborative Research:				
4.a	Collaborative research with PSIT will continue during the third year of the CIT project.	2-15-92	2-15-92		

3.4 Liquefaction Reactivity of Low-Rank Coals

LIQUEFACTION REACTIVITY OF LOW-RANK COALS

Semiannual Technical Progress Report
for the Period January - June 1992

by

Edwin S. Olson, Research Supervisor
Ramesh K. Sharma, Research Associate

Energy and Environmental Research Center
University of North Dakota
Box 8213, University Station
Grand Forks, ND 58202

Technical Monitor: Udaya S. Rao

for

U.S. Department of Energy
Pittsburgh Energy Technology Center
626 Cochran Mill Road
Pittsburgh, PA 15236

July 1992

Work Performed Under Cooperative Agreement No. DE-FC21-86MC10637

TABLE OF CONTENTS

	<u>Page</u>
LIST OF TABLES	ii
1.0 EXECUTIVE SUMMARY	1
2.0 GOALS AND OBJECTIVES	2
3.0 ACCOMPLISHMENTS	2
3.1 Introduction	2
3.2 Experimental	3
3.2.1 Instrumentation	3
3.2.2 Catalytic CO/Water Liquefaction of Coal	3
3.2.3 Catalytic CO/Water Reactions of Model Compounds	4
3.3 Results and Discussion	5
3.3.1 Catalytic CO/Water Liquefaction of U.S. Coals	5
3.3.2 CO/Water Reactions of Model Compounds	7
3.3.2.1 Catalytic Hydrogenation of Polynuclear Aromatic Hydrocarbons	8
3.3.2.2 Catalytic Reduction of Ketones	11
3.3.2.3 Catalytic Hydrocracking of Model Compounds	13
3.3.2.4 Catalytic Decarboxylation of Carboxylic Acids	15
4.0 REFERENCES	17

LIST OF TABLES

<u>Table</u>		<u>Page</u>
1	Catalytic Liquefaction of Coals	4
2	CO/Water Hydrogenation of Polynuclear Aromatic Hydrocarbons	9
3	CO/Water Conversions and Electron Affinities of Polynuclear Aromatics	10
4	CO/Water Reductions of Anthrone	12
5	CO/Water Reduction of Ketones	12
6	CO/Water Hydrocracking of Model Compounds	14
7	CO/Water Reactions of Naphthoic Acid	15
8	CO/Water Reactions of Substituted Carboxylic Acids	16

LIQUEFACTION REACTIVITY OF LOW-RANK COALS

1.0 EXECUTIVE SUMMARY

Coal liquefaction has been effectively carried out in a number of laboratories with carbon monoxide reductant in an aqueous solvent (CO steam process). Catalysts are sought which could improve the conversion in the process and avoid the high pressures required. Australian workers demonstrated that sodium aluminate is able to catalyze the conversion of Australian coals in the CO/water system and in water/hydrogen donor solvent mixtures. The Energy and Environmental Research Center (EERC) project has focused on demonstrating an economical process for the liquefaction of low-rank coal, and aqueous sodium aluminate has been utilized as the catalyst. High conversions comparable with those obtained with hydrogen donor solvents and hydrogen sulfide were obtained. The product consists of a large distillate fraction composed of oxygenated compounds and many aromatics. The asphaltene and oil fractions are suitable for second-stage catalytic hydrogenation. Reactions utilizing hydrogen as the reductant gave low conversions with sodium aluminate.

The use of a mixed solvent system for the CO reduction was investigated. A solvent composed of water and tetralin gave somewhat lower conversion with the Wyodak coal, but the pressure was lowered by a large factor. Hydrogen was donated to the coal from the tetralin as well as from the water. Substituting an aromatic solvent or an alcohol solvent for the hydroaromatic tetralin gave lower conversions.

CO/water reductions of Blind Canyon bituminous coal in both water and water/tetralin mixture were also successful, but less so than the reactions of the Wyodak coal.

An understanding of how carbon monoxide reduces coal in this first-stage liquefaction process is essential for implementing improvements to the process and for designing effective catalysts. The reductive reactions catalyzed by the sodium aluminate in aqueous/carbon monoxide systems were investigated with various model compounds in order to learn more about the structure-reactivity parameters that may elucidate the nature of this reduction.

Reactions of polycyclic aromatic hydrocarbons in the CO/water/ NaAlO_2 system showed that those aromatics with linear arrangement (annellation) of the polycyclic rings are readily converted to hydroaromatics. The reactivities of the aromatics correlate with the ability to accept electrons (electron affinity) and form the radical anion intermediate. There also appears to be a reactivity factor involving addition of protons to the radical anion intermediate. Similar effects were noted for a series of aromatic ketones. The role of the sodium aluminate may involve forming a complex with the carbon monoxide that can more effectively donate electrons in the reaction. The effect of the sodium aluminate is not large, but it may be very important in optimizing the conversion of coal aromatic structures into hydroaromatic and other alkyl-bridged structures that are important in subsequent thermal or catalytic reactions.

Very great conversion effects for the sodium aluminate component were noted in the reactions of model carboxylic acids in the CO/water system. The nature of this catalytic effect is still under investigation. Evidence for a very large synergistic effect on diaryl ether hydrolysis was discovered for the combination of sodium aluminate with carboxylic acid groups.

2.0 GOALS AND OBJECTIVES

The efficient production of environmentally acceptable distillate fuels requires catalysts for hydrogenation and cleavage of the coal macromolecule and removal of oxygen, nitrogen, and sulfur heteroatoms. Currently, two-stage processes for coal conversion are under development. The first stage converts coal to a soluble form with minimal cracking and hydrogenation. This processing presently involves no catalyst other than the coal mineral matter present and the addition of a promoter, hydrogen sulfide, which may have a catalytic effect. The second stage involves hydrogenation upgrading of the first-stage product to distillates with fixed- or ebullated-bed catalysts.

The catalysts currently used in the second stage of coal liquefaction for hydrotreating the first-stage product are the same as those used in conventional petroleum refining; however, this application has not been very successful. Improvements in upgrading efficiency could be obtained if catalysts with longer life and better activity and selectivity were available. Rapid deactivation of the conventional Co-Mo and Ni-Mo catalysts on an alumina support have been attributed to coke formation (1), metals deposition (2), and inhibition of the active center by chemisorbed compounds (3). The objectives of this research project are to develop and test novel heterogeneous catalysts for hydrotreatment upgrading of first-stage coal liquefaction products. The new hydrogenation catalysts are based on pillared clays and hydrotalcites, which have very large micropore dimensions to accommodate the coal macromolecule, but yet do not possess strong acidities which lead to coking at high temperatures. A second objective is to develop a solid acid catalyst for depolymerization of the coal macromolecule. The acid catalysis process for coal liquefaction is believed to operate by ionic mechanisms. Some molten acids have successfully depolymerized coal, but the poor efficiencies of catalyst recovery and the corrosive nature of the catalyst make the process uneconomical. Stable solid acid catalysts will be developed which will avoid these difficulties. These catalysts are also based on pillared clays as well as on silica bases.

3.0 ACCOMPLISHMENTS

3.1 Introduction

The development of new catalysts for coal liquefaction was continued. The catalysts currently being investigated are basically homogeneous catalysts for first-stage coal solubilization and preliminary reduction.

Catalysis of the first stage of coal liquefaction involves improving the rates of bond cleavage reactions leading to improved solubility and of preliminary reduction reactions so that oils and asphaltene are produced without extensive retrogressive reactions. These materials should be able to

effectively interact with the solid and colloidal coal matter, catalyzing the conversion to soluble oils at moderate temperature, while minimizing problems with low surface areas or mass transfer. Thus various inorganic agents that are soluble in the reaction vehicle or solvent are being investigated. Some of these (e.g., sodium aluminate) are polymeric at the reaction conditions and are precursors for the clays and zeolites that are currently under investigation as second-stage liquefaction catalysts.

3.2 Experimental

The reagents bibenzyl, diphenyl sulfide, diphenyl ether, naphthalene, phenanthrene, anthracene, pyrene, fluoranthene, 1,2-benzanthracene, 2,3-benzanthracene, triphenylene, perylene, acetophenone, benzophenone, 1-acetonaphthone, 9-acetylanthracene, anthrone, benzanthrone, 1-methylnaphthalene, 1-naphthoic acid, and 2-phenoxybenzoic acid were obtained from Aldrich.

3.2.1 Instrumentation

Quantitative GC/FID analyses were performed with a Hewlett Packard 5880A gas chromatograph equipped with a Petrocol capillary column. A mixture of isooctane and n-octadecane was the internal standard. GC/FTIR/MS was performed on a Finnigan 800 ITD ion trap detector with a HP 5890A gas chromatograph and a J&W 30-m x 0.32-mm (ID), 1.0-micron film of DB-5. A 15-m x 0.25-mm (ID), 0.25-micron DB-5 film capillary column was used for the analysis of high boiling components.

3.2.2 Catalytic CO/Water Liquefaction of Coal

A slurry consisting of 5.0 g of coal (as received Wyodak-Clovis Point) and a solution of the catalyst in 20 g of water was placed in a 70-mL Parr reactor. The reactor was evacuated and charged with a mixture of 1000 psi of desired gas. The reactor was heated to 400°C in a rocking autoclave (initial heatup time = 11 minutes) and left at this temperature for 30 minutes. At the end of the reaction, the reactor was cooled to room temperature, and the gases were removed. The reactor was attached to a set of two traps cooled in ice and liquid nitrogen. The product slurry was distilled to remove water and other volatile components. The distillate was saturated with NaCl and extracted with ether. The extract was mixed with the internal standards and analyzed by GC and GC/FTIR/MS. The residue from distillation of the water and volatiles was extracted with pentane, toluene, and tetrahydrofuran (THF). The pentane-soluble fraction was mixed with an internal standard and analyzed by GC. The toluene-soluble, THF-soluble, and THF-insoluble fractions were dried in vacuo at 110°C overnight and weighed. The weight of mineral matter and catalyst were subtracted from the dry weight of the THF-insoluble fraction to obtain the maf weight of unconverted coal, which was used in the calculation of percent conversion. The conversion to soluble material and the product fraction yield data are given in Table 1.

The workup procedure for the mixed water/organic solvent system was different in that the distillation was omitted, and pentane was added directly to the reaction product slurry. The slurry was thoroughly extracted with pentane and separated into the pentane-soluble fraction that included the organic solvent and the residue that included the water phase. The residue

TABLE 1
Catalytic Liquefaction of Coals

Reaction Temp. = 400°C, Reaction Time = 30 min Reductant gas (CO) = 1000 psi (at room temp.)						
Catalyst (mmol/g coal)	Coal (AR) (g)	Solvent(s) (g)	Conv.* (%)	Products (%)		
				Tol-S	THF-S	Pent-S**
NaAlO ₂ (0.5)	Wyodak (5.0)	Water (20.0)	89	20	27	42
NaAlO ₂ (0.5)	Wyodak (5.0)	Tetralin (5.2) Water (3.5)	79	19	30	30
NaAlO ₂ (0.5)	Wyodak (5.0)	1-MeNaph (5.0) Water (3.5)	71	11	27	33
NaAlO ₂ (0.5)	Wyodak (5.0)	Ethanol (5.1) Water (3.5)	75	14	28	33
NaVO ₃ (0.5)	Wyodak (5.0)	Tetralin (5.0) Water (3.5)	72	14	30	27
NaAlO ₂ (0.5)	Blind Canyon (5.3)	Water (20.0)	47	5	30	12
NaAlO ₂ (0.5)	Blind Canyon (5.4)	Tetralin (5.4) Water (3.6)	58	14	25	19

* = Conversions are based upon the amount of initial coal (maf).

** = Pentane solubles are by difference, also includes the products extracted by ether from the distillate.

was extracted with toluene, then THF as above. The water was extracted into the THF and was removed along with the THF by rotary evaporation.

In the workup of the experiment with the water/ethanol system, the initial extraction of the product slurry was carried out with toluene, and then pentane was added to the toluene extract to obtain the pentane-soluble fraction and the toluene-soluble (pentane-insoluble) fraction.

3.2.3 Catalytic CO/Water Reactions of Model Compounds

In a typical run, 0.5 g of model compound, 2 g of solvent(s), and the desired amount of catalyst were placed in a tubing bomb (12-mL microreactor). The microreactor was evacuated, pressurized with 1000 psig of carbon monoxide, placed in a rocking autoclave, and heated to 400°C. At the end of the

specified reaction period, the microreactor was cooled in a dry ice-acetone slurry, degassed, and opened. In the experiments with carboxylic acids, the resulting slurry was acidified with dilute HCl to convert any remaining carboxylate salts to the acid form. The desired amount of the internal standard was added to the product slurry, and the product slurry was extracted with dichloromethane or chloroform (for perylene and 2,3-benzanthracene products). The extract solution was dried over molecular sieves (4 Å) and analyzed by GC/FID and GC/FTIR/MS.

3.3 Results and Discussion

3.3.1 Catalytic CO/Water Liquefaction of U.S. Coals

In the first part of our study of homogeneous catalysts for first-stage coal liquefaction, catalysts for improving the conversion and product quality of liquefactions carried out in aqueous systems were investigated. Aqueous reactions that utilize carbon monoxide as the reductant gas have been extensively investigated in this and other laboratories over many years (4-6). Basic catalysts have been employed to achieve higher conversions. The aqueous/CO reduction has been shown to be superior to hydrogen for the first stage of liquefaction.

In screening a number of candidates for improving the conversion in aqueous/CO liquefaction processing, Jackson and others (7,8) found that aqueous sodium aluminate gave good conversions of brown coal to oils at temperatures of 350° to 400°C. Factors such as pH and concentration in aqueous systems of the materials are critical in determining the actual aluminate structures present (monomeric or polymeric); however, Jackson did not report the pH of his system. The sodium aluminate in some form could activate the carbon monoxide so as to produce an electron-, hydride-, or hydrogen-donating intermediate that would be a more effective reducing agent than the carbon monoxide without promoter.

Previous results have shown that the addition of sodium aluminate to the CO-water system improves the conversion of Wyodak subbituminous coal to distillate and soluble products at 400°C (9). In the current reporting period, the reactions of Wyodak and Blind Canyon coals with aqueous CO were conducted under various conditions to investigate the role of catalyst as well as solvent in determining the quality and yields of the liquefaction products. The reaction conditions and yield data are given in Table 1. Since high conversions to THF solubles are easily obtained at 400°C without any promoter or catalyst with the low-rank coals, the conversion to oils, asphaltenes, and distillate was accurately determined to evaluate the activity of sodium aluminate.

The conversion of Wyodak subbituminous coal to THF solubles in the aqueous/CO liquefaction with sodium aluminate was 89% (Table 1). This was substantially higher than that obtained with no added sodium aluminate (9). The high conversion with sodium aluminate is consistent with that observed by Jackson and others for Australian brown coals (7,8).

The composition of the distillate, oil, and asphaltene product obtained after first-stage liquefaction of Wyodak coal in aqueous CO was determined for comparison with that obtained previously in organic solvents with CO or with

hydrogen. These studies indicated that the volatile first-stage product from aqueous liquefaction contained large amounts of phenolics rather than hydrocarbons. This result offers the possibility in coal processing of removing the distillate and using it elsewhere, so that hydrogen needed for liquefaction is not wasted in deoxygenation of phenols.

Reactivity data for some other coals in CO/water/ NaAlO_2 were desired. Conversion of Blind Canyon (high volatile bituminous) coal with sodium aluminate catalyst was much lower than that of the Wyodak coal. Only 47% of the Blind canyon coal was converted to THF-soluble products under the same conditions. Tests with other coals will be carried out in the next year.

Sodium aluminate-catalyzed liquefaction of coals in the CO/water system is very effective, but high pressures are developed in the reactor. In order to lower the operating pressure, liquefaction of coal was conducted using a mixture of tetralin and water. Mixed solvent liquefaction of Wyodak coal was carried out by heating a well-mixed slurry of coal in aqueous sodium aluminate plus tetralin (5-g as-received coal/5-g tetralin/3-g water/2.5 mmol of sodium aluminate) for 30 minutes at 400°C in the presence of 1000 psig initial CO pressure. Compared with the CO/water system, CO/water/tetralin gave somewhat lower conversion (79%). The lower conversion could be related to the lower pressure. The pressure is below the critical pressure of the water, and different properties of the solvent, as well as of the solute species, would be expected.

In contrast, the use of a mixed solvent in the liquefaction of Blind Canyon bituminous coal with sodium aluminate catalyst significantly improved the conversion (58%) compared with the liquefaction in water solvent (Table 1). However, the conversion is still lower than that obtained with Wyodak subbituminous coal. This result indicates that there may be complex phase problems with regard to the solvents, and each coal will require experimentation to determine optimum solubilization parameters.

Current liquefaction processes generally utilize a hydrogenated recycle solvent containing hydroaromatics that could serve as hydrogen donors. The tetralin used in the experiments above was intended to model this behavior. However, a nonhydrogenated solvent could be used in processing if it gave equivalent conversions and product quality in the CO/mixed water-organic solvent liquefaction. In order to determine the effects of the type of organic solvent on yields and product quality in mixed water-organic solvent liquefaction, the reactions of Wyodak coal were carried out in mixed solvents composed of water plus 1-methylnaphthalene and water plus ethanol, under reaction conditions similar to the water/tetralin reaction described above. Sodium aluminate-catalyzed liquefaction of Wyodak coal in water/1-methylnaphthalene and water/ethanol solvent systems gave 71% and 75% conversions, respectively. Compared with the water/tetralin system, water/1-methylnaphthalene and water/ethanol gave lower conversions. It should also be pointed out that in the water/tetralin system, some of the tetralin was converted to naphthalene (see discussion below); thus the tetralin played some role in hydrogenating, donating hydrogens to the first-stage liquefaction product. The reduced yields obtained with the aromatic and alcohol solvents mean that better results will probably be obtained in a process that uses a hydrogenated recycle solvent, as in the current Wilsonville art.

The liquefaction product quality as determined by the distribution of solubility fractions was good for the sodium aluminate-catalyzed reaction. As shown in Table 1, the toluene solubles amounted to 20% of the maf coal, and 42% of the coal was converted pentane solubles, CO₂, and H₂O. The major products in the distillate were oxygenated compounds, such as methanol, 2-propanol (from acetone), and phenolics. In addition, there were hundreds of hydrocarbon components that are typically found in coal-derived products. However, the reaction in the water/tetralin system gave a significantly lower yield of pentane-soluble products. Yields of toluene and THF-soluble materials were comparable. The amount of phenol was slightly lower, but the amounts of alkylphenols were significantly higher. Total phenolics amounted to ca. 6% of the starting maf weight of coal.

The composition of the solvent and solvent-derived species was determined for the water/tetralin liquefaction experiments to define the role of the hydroaromatic solvent, if any, in the first-stage process. The ratio of tetralin/naphthalene was 20, indicating that approximately 5% of the tetralin was converted into naphthalene. This means that hydrogen transfer from tetralin occurs during liquefaction. A large number of alkyltetralins and alkyl naphthalene were also found, probably some by addition to the solvent and some from depolymerization of the coal.

Reactions in water/1-methylnaphthalene gave significantly lower conversion to toluene-soluble products. Thus the effect of the reaction solvent on the product appears to be related more to the higher molecular weight species, increasing their solubility by hydrogen donation or adduction. Compared with water/tetralin solvents, the amount of phenol was lower, but the amount of alkylphenols was significantly higher for the water/1-methylnaphthalene solvent. A large number of alkyl naphthalenes were formed.

The reaction of Wyodak coal in water/ethanol gave a product distribution similar to that obtained from the water/1-methylnaphthalene system. However, the amount of phenol and cresols was significantly lower than that obtained from water only or water/tetralin and water/1-methylnaphthalene reactions. This is perhaps due to the mineral-catalyzed conversion of phenolics to ethylphenols in the supercritical ethanol.

Compared with Wyodak coal, sodium aluminate-catalyzed liquefaction of Blind Canyon coal gave a very low conversion to toluene- and pentane-soluble products. The water/tetralin solvent system significantly improved the conversion to toluene and pentane-soluble materials, whereas the yield of THF-soluble material decreased. Analysis of the pentane-soluble materials from calibrated GC data indicated that only 2% of the coal was converted to phenolic materials. Based on the retention time of the components, it is concluded that Blind Canyon (bituminous coal) produced higher molecular weight products than the Wyodak subbituminous coal during CO/water liquefaction.

3.3.2 CO/Water Reactions of Model Compounds

An understanding of how carbon monoxide reduces coal in first-stage liquefaction is essential for implementing improvements to the process and designing effective catalysts. Why does CO give better conversions to soluble materials than hydrogen? After several decades, little is understood about the mechanism of the aqueous CO reaction with coal or even with model organic

compounds. Jones and others have shown that an aryl ketone (benzophenone) and an aryl carbinol are reduced (10). Bases were required for reduction of the ketone, and higher conversions were obtained for the carbinol reduction in the presence of base. Reduction of anthracene and quinoline were also effected with aqueous CO; however, higher conversions of anthracene were obtained in the absence of base (11). The reduction of ketones with CO in aqueous sodium carbonate was explained by sodium ion activation of the CO to give an intermediate such as formate that can donate hydride to the carbonyl. Reduction of anthracene or other hydrocarbons would appear to proceed by a different mechanism.

The second priority in our program was to understand something about the activation of CO and the nature of the sodium aluminate catalysis. Sodium aluminate could probably activate CO for hydride reduction of ketones as well as sodium carbonate, perhaps better. But does it also activate CO so that hydrogenation of hydrocarbons occurs? Can it lower activation energies for cleavage of bonds such as in ether and carboxylate groups? The reactions of several model compounds were investigated in aqueous/CO conditions, and the results were compared with those obtained in the absence of the sodium aluminate.

3.3.2.1 Catalytic Hydrogenation of Polynuclear Aromatic Hydrocarbons

Naphthalene, anthracene, phenanthrene, pyrene, fluoranthene, triphenylene, perylene, 1,2- and 2,3-benzanthracene were used as test compounds to investigate the hydrogenation of a polynuclear aromatic system by an aqueous CO system (Table 2).

Naphthalene was not reduced by the CO/water system at 400°C with or without the addition of sodium aluminate catalyst. In contrast, anthracene was quite reactive under these conditions, as described in the previous report (9). This earlier work demonstrated that higher conversions of anthracene were obtained with sodium aluminate than without this catalyst. But lower conversions were obtained with sodium hydroxide, which was consistent with the results Stenberg reported for reactions with a similar base, sodium carbonate, at higher temperatures.

The conversion data for other polynuclear aromatic compounds, which were obtained in this quarter (Table 2), further demonstrated a wide divergence in reactivity. Phenanthrene, pyrene, fluoranthene, and perylene were not very reactive. Thus additions of rings (annellations) to the naphthalene structure that are nonlinear do not significantly increase the reactivity, but linear benzannellation, as in the anthracene structure, results in a significant increase in reactivity.

This structural effect on reactivity of the polynuclear aromatics is further demonstrated in the benzanthracene series. 2,3-Benzanthracene, which contains the linear polynuclear aromatic system, gave a very high (94%) conversion to the dihydrogenated product. The nonlinear benzannellated isomer, 1,2-benzanthracene, was less reactive (10% conversion) than anthracene. Thus the effect of linear versus nonlinear benzannellation on the

TABLE 2

CO/Water Hydrogenation of Polynuclear Aromatic Hydrocarbons

Reaction Temp = 400°C, Reaction Time = 2 hr Reductant (CO) = 1000 psi			
Catalyst (mmol/g substr)	Substrate (mmol)	Conv. (%)	Major Products (mmol)
NaAlO ₂ (0.50)	Naphthalene (3.90)	<1	Tetralin (trace)
NaAlO ₂ (0.50)	Anthracene (2.77)	82	9,10-Dihydroanthracene (2.19) Tetrahydroanthracene (0.13)
NaAlO ₂ (0.5)	Phenanthrene (2.81)	2	Dihydrophenanthrene (trace)
NaAlO ₂ (0.5)	Pyrene (2.52)	4	Dihdropyrene (0.04) Tetrahydropyrene (0.01)
NaAlO ₂ (0.50)	1,2-Benzanthracene (0.44)	10	Dihydro 1,2-Benzanthracene (0.04)
NaAlO ₂ (0.50)	2,3-Benzanthracene (0.44)	94	Dihydro 2,3-Benzanthracene (0.36)
NaAlO ₂ (0.50)	Fluoranthene (2.47)	<1	None
NaAlO ₂ (0.50)	Perylene (0.40)	3	Hydroperylenes (trace)

reactivity behavior in the anthracene series is consistent with that reported above for other aromatics.

These reactivity data suggest that certain (linear) aromatic structures in coals might be expected to be reduced in a first-stage liquefaction process that uses CO as the reducing gas. Although "deep" reduction of aromatics does not proceed, hydrogen is added at critical sites in the structures, and the resulting hydroaromatic structures may be effective in promoting further reactions such as radical capping and in preventing retrograde reactions that may occur during thermal processing. The effects of substituents on the reactivity of the aromatics were not studied, but since reactivities are usually affected significantly by substituents, especially heteroatoms, the reduction of these types of structures in coal in the catalytic CO/water system is even more likely.

Correlations of the reactivity data with other chemical properties of the polynuclear aromatics may also provide important clues as to the nature or mechanism of the CO/water reduction. The high reactivity of anthracene and other linear polynuclear aromatics in the reduction reaction suggests that a relationship of the observed reactivity of the aromatic hydrocarbon with the electron affinity (EA) of the hydrocarbon may be significant. The reaction of the aromatic compounds with the reducing agent (CO or complexed CO) may

transfer a single electron to initially form a radical anion intermediate. The most reactive aromatics would be those with the highest electron affinities. Since various methods have been used for determining electron affinities, various compilations of electron affinities exist with different values. In Table 3 the electron affinities of various polynuclear aromatics are reported along with the corresponding conversions in the CO/water/NaAlO₂ system. Values for cathodic reduction potentials ($E_{1/2}$) are also available and are listed in Table 3.

Aromatic compounds with positive electron affinities have a low-energy lowest unoccupied molecular orbital (LUMO) for accepting an electron. Because of the relatively high LUMO energies for benzene and naphthalene, the electron affinities for unsubstituted benzene and naphthalene are low or negative, depending on the type of measurement; hence, under some conditions, the corresponding radical anions are unstable. More highly conjugated or substituted aromatics will have a lower-energy LUMO and, consequently, have positive electron affinities.

Although a regression analysis has not been performed, there appears to be a correlation of the conversion data with the EA values determined from the lowest-energy UV band (12,13). The low reactivities for naphthalene, phenanthrene, triphenylene, and pyrene are correctly predicted from the low EA values. The high reactivities for anthracene, 2,3-benzanthracene, and 1,2-benzanthracene are also predicted in the correct order. Only the perylene EA value does not seem to be consistent with the low reactivity observed in the CO/water system. The EA values from the 0-0 transition (13) for naphthalene, anthracene, phenanthrene, and triphenylene also appear to correlate with the reactivities, but the EA values of pyrene, perylene, and 1,2-benzanthracene are too large for the observed reactivities of these compounds in this system. Other EA values calculated from molecular orbital theory are also consistent with the observed reactivities (14). The half-wave reduction potentials ($E_{1/2}$) of the aromatic compounds (15) do not appear to

TABLE 3

CO/Water Conversions and Electron Affinities of Polynuclear Aromatics

Substrate	Conv.	EA (12,13)	EA (13)	EA (14)	$E_{1/2}$ (15)
Naphthalene	<1	-0.40	-0.12	-0.38	1.98
Anthracene	82	0.50	0.42	0.49	1.46
Phenanthrene	2	-0.31	0.20	-0.20	1.94
Triphenylene		-0.41	0.14	-0.28	1.97
Pyrene	4	0.09	0.39	0.68	1.61
Fluoranthene	<1				1.35
Perylene	3	0.75		0.80	1.25
1,2-Benzanthracene	10	0.29	0.46	0.62	1.53
2,3-Benzanthracene	94	0.92	0.98	0.82	1.14

give as good a correlation with the reactivities. This may be due to additional surface and solvent effects that occur during the electrode potential measurements.

A process involving single electron transfer (SET) from CO or a CO aluminate complex to the aromatic substrate is consistent with the reactivity data. With some aromatic compounds, the resulting radical anion may react rapidly with water or hydroxyl such that a hydrogen ion (H^+) is transferred. The rate of this protonation reaction may differ considerably for the various anion radical intermediates. In fact, the rate constants for protonation of perylene and fluorene radical anions are much lower than those of other aromatics (16). This may explain their lack of reactivity in the CO/water reduction tests discussed above. As in some other SET reactions, the hydrogen ion could begin bonding synchronously with the electron transfer in the more reactive aromatics (17). The radical resulting from the H^+ transfer will then react further with an electron donor to give the carbanion intermediate which is again protonated. Further study of structure-reactivity data is needed to refine the SET concept for CO/water reductions.

The nature of the complexation products of CO with metal oxides has been investigated under anhydrous conditions (18,19). These surface bound species exhibit spectra consistent with dimeric or polymeric structures which may be paramagnetic. The structures of CO/metal oxide complexes present in high-temperature hydrous conditions are unknown, but the possibility exists that the unpaired electrons on the CO ligand are involved in SET reduction of the aromatic compounds.

3.3.2.2 Catalytic Reduction of Ketones

The reactions of ketones with CO/water were also investigated as models for possible reactions that would occur in coal liquefaction (Tables 4 and 5). Since most of the aryl ketones have a high electron affinity, the reaction temperature was reduced to 350°C, so that structure-reactivity effects could be more easily distinguished.

The reduction of anthrone in CO/water with sodium aluminate catalyst was slightly greater than in the reaction without sodium aluminate. The major products were anthracene and dihydroanthracene. The intermediate alcohol reduction product (anthrol) was not obtained, because it very rapidly dehydrates to anthracene. Dihydroanthracene could have formed by reduction of anthracene, which occurs readily (see discussion above), or possibly by reduction of a carbonium ion intermediate that forms when the alcohol intermediate eliminates hydroxyl.

The reduction of anthrone was also carried out in the mixed water/tetralin solvent system. The conversion decreased by 10%, which is consistent with the decrease observed in the coal conversion in the same solvent system. The decrease can be attributed to either the lower pressure of the system, which results in lower concentration of electron donor (CO complex), or to a phase separation problem that is not currently understood.

The amount of benzophenone converted to reduced products with sodium aluminate catalyst was similar to that found for anthrone (53%). The reduction products are quite different in nature, however. The alcohol

TABLE 4

CO/Water Reductions of Anthrone

Reaction Temp. = 350°C, Reaction Time = 2 hr Reductant (CO) = 1000 psi				
Catalyst (mmol/g substr)	Substrate (mmol)	Solvent (g)	Conv. (%)	Major Products (mmol)
None	2.58	Water (2.01)	49	Anthracene (0.57) Dihydroanthracene (0.35)
NaAlO ₂ (0.50)	2.58	Water (2.04)	52	Anthracene (0.62) Dihydroanthracene (0.39)
NaAlO ₂ (0.50)	2.58	Water (0.3) Tetralin (0.5)	42	Anthracene (0.33) Dihydroanthracene (0.30) Tetrahydroanthracene (0.02)

TABLE 5

CO/Water Reduction of Ketones

Reaction Temp. = 400°C, Reaction Time = 2 hr Solvent (water) = 2 g, Reductant (CO) = 1000 psi				
Catalyst (mmol/g substr)	Substrate (mmol)		Conv. (%)	Major Products (mmol)
None	Benzophenone (2.64)		37	Diphenylmethane (0.70) Benzhydrol (0.22)
NaAlO ₂ (0.50)	Benzophenone (2.70)		53	Diphenylmethane (0.94) Benzhydrol (0.46)
NaAlO ₂ (0.5)	Acetophenone (4.17)		55	Ethylbenzene (0.36) Styrene (0.66) 1-Phenylethanol (0.73) Phenol (0.06) Benzene (trace) Toluene (trace)
NaAlO ₂ (0.50)	1-Acetonaphthone (3.00)		53	1-Ethyl-naphthalene (0.68) 1-Vinyl-naphthalene (0.52) 1-Methyl-naphthalene (0.05) Naphthalene (0.03) 1(1-naphthyl) ethanol (0.13)
NaAlO ₂ (0.50)	9-Acetylanthracene (0.45)		77	Anthracene (0.17) Dihydroanthracene (0.13) Ethylanthracene (0.03)
NaAlO ₂ (0.50)	9-Fluorenone (0.60)		89	Fluorene (0.26) 9-Fluoreno1 (0.18)
NaAlO ₂ (0.50)	Benzanthrone (2.16)		100	Dihydrobenzanthrone (2.00)

product (benzhydrol) was present, since it does not eliminate hydroxyl to form a stable aromatic compound as in the anthrone system. Instead, elimination of hydroxyl resulted in reduction to diphenylmethane. The reduction of benzophenone in the absence of sodium aluminate was lower than that observed for anthrone.

The conversion of fluorenone to reduced products was substantially higher than observed for anthrone. About the same ratio of alcohol to methylene product was found. The more favorable electron affinity is due to the higher stability of the fluorenyl anion system. A low-energy LUMO is also present in the polycyclic benzanthrone, which was completely reduced by the CO/water/ NaAlO_2 system.

A comparison of the reactivity of the series of aryl methyl ketones was also conducted with interesting results. Reduction of a single aryl ring ketone (acetophenone) was effected in 55% conversion to give a mixture of products. The intermediate alcohol was present, and this product was further converted to styrene via elimination of the hydroxyl group. Besides the styrene, a substantial amount of ethylbenzene was formed. Reduction to the methylene could have occurred via the intermediate carbonium ion or perhaps by reduction of styrene.

Acetonaphthone exhibited a similar reactivity, giving 52% conversion to a similar mixture of products. As expected, the ketone group was reduced, and the naphthalene rings were not reduced, owing to the low electron affinity of the naphthalene system. In addition to the alcohol, vinylnaphthalene, and ethylnaphthalene, a very small amount of methylnaphthalene and naphthalene were formed. 9-Acetylanthracene gave a high conversion (77%) to products. In this case, the more easily reduced anthracene moiety generated some additional reaction pathways, including hydrocracking of the aryl-alkyl bond. Ethylanthracene from reduction of the aceto group was a minor product. Anthracene was major product, which may have formed via elimination of the ethyl group from the intermediate radical, 10-hydro-10-ethyl-9-anthracenyl. Anthracene was then further reduced to dihydroanthracene.

The results of the model ketone reductions suggest that the CO/water/ NaAlO_2 reduction of coals that are believed to contain significant amounts of aryl ketones will also produce significant reduction to less oxygenated and perhaps hydroaromatic structures. The presence of these structures may significantly lower the tendency of coal materials to undergo retrograde condensation reactions during further thermal and catalytic cracking reactions. Further work with quinones is planned so that we can determine whether the products from these reactions with CO/water will also be less likely to participate in the retrograde reactions.

3.3.2.3 Catalytic Hydrocracking of Model Compounds

The hydrocracking activity of the sodium aluminate-catalyzed CO/water system was investigated using bibenzyl, diphenyl sulfide, and diphenyl ether as the test compounds. The reaction of bibenzyl was carried out at 425°C for 2 hours with aqueous sodium aluminate in the presence of 1000 psig initial CO pressure. A higher temperature was used, since the amount of hydrocracking observed in the studies discussed above was very small at those temperatures. The conversion data are given in Table 6. The conversion of bibenzyl was 37%,

TABLE 6
CO/Water Hydrocracking of Model Compounds

Reaction Temp. = 425°C, Reaction Time = 2 hr Solvent (water) = 2 g, Reductant (CO) = 1000 psi				
Catalyst (mmol/g substr)	Substrate (mmol)	Temp. (°C)	Conv. (%)	Major Products (mmol)
NaAlO ₂ (0.5)	BB (2.78)	425	37	Benzene (0.21) Toluene (0.35) Ethylbenzene (0.15)
None	DPE (2.90)	350	2	Benzene (trace)
NaAlO ₂ (0.50)	DPE (2.29)	350	3	Benzene (trace)
None	DPS (2.78)	425	18	Benzene (0.54)
NaAlO ₂ (0.50)	DPS (2.74)	425	28	Benzene (0.70)

BB = Bibenzyl.
DPE = Diphenyl ether.
DPS = Diphenyl sulfide.

which is comparable with sodium carbonate-catalyzed reactions (20). The major products were benzene, toluene, and ethylbenzene. Stenberg and coworkers have investigated the reduction of bibenzyl using sodium carbonate, alkaline earth oxides, and fly ash as disposable catalysts in carbon monoxide-water systems (20).

Stenberg and coworkers reported that CO-water effectively cleaves aryl-sulfur bonds in diphenyl sulfide (64.4% conversion) at 425°C in CO-water for a 2-hr reaction. Addition of sodium carbonate results in lower conversion (47%) of diphenyl sulfide (21). However, we found conversions of only 18% for diphenyl sulfide in reactions without sodium aluminate under the above conditions. Addition of sodium aluminate significantly improved the cleavage of the aryl-sulfur bond as indicated by 28% conversion. Benzene was the only reaction product.

The reaction of diphenyl ether in CO-water with and without sodium aluminate was carried out at 350°C for 2 hours in the presence of 1000 psi of initial CO pressure. The results indicated that CO-water both with and without sodium aluminate promoter did not cleave the aryl-oxygen bond.

3.3.2.4 Catalytic Decarboxylation of Carboxylic Acids

The decarboxylation of carboxylic acids was investigated by using carboxylic acid substrates, 2-benzylbenzoic acid (2-BBA), 2-phenoxybenzoic

acid (2-PBA), and 1-naphthoic acid as the test compounds to determine if there are any catalytic effects on decarboxylation or other reactions that might occur on heating carboxylic acids. Reactions of these compounds were carried out at 350°C for 2 hours in the presence of 1000 psi of CO initial pressure. Reactions of 1-naphthoic acid were also conducted at 300°C. Due to analytical difficulties in accurately determining the amount of carboxylic acids, the product yield was used to determine percent conversion of the carboxylic acids. Reaction conditions and conversion data are given in Table 7.

The reaction of naphthoic acid in CO-water gave 10% and 18% conversions of 1-naphthoic acid into products at 300° and 350°C respectively. The major product was naphthalene. The addition of sodium aluminate increased the conversion to 17% and 37% for 300° and 350°C reactions, respectively. The dramatic catalytic effect of the sodium aluminate on decarboxylation may have a very important role in first-stage liquefaction, and more efforts to understand this effect are in progress. In addition to naphthalene (major product), trace amounts of tetralin were also formed in the sodium aluminate-catalyzed reactions. It is not known whether the naphthalene reduction

TABLE 7
CO/Water Reactions of Naphthoic Acid

Reaction Time = 2 hr, Reductant (CO) = 1000 psi					
Catalyst (mmol/g substr)	Substr. (mmol)	Temp. (°C)	Solvent (g)	Conv. (%)	Major Products (mmol)
None	2.95	300	Water (2.10)	10	Naphthalene (0.17)
NaAlO ₂ (0.50)	2.92	300	Water (2.02)	17	Naphthalene (0.23) Tetralin (trace)
NaOH (0.50)	2.80	300	Water (2.00)	9	Naphthalene (0.12)
NaAlO ₂ (0.50)	2.81*	300	Water 2.00	12	Naphthalene (0.16)
None	0.70	350	Water (2.02)	18	Naphthalene (0.12) Tetralin (0.01)
NaAlO ₂ (0.50)	0.70	350	Water (2.00)	37	Naphthalene (0.18) Tetralin (0.01)
NaAlO ₂ (0.5)	0.70	350	Water (0.30) Tetralin (0.50)	19	Naphthalene (0.31) Tetralin (3.6)
NaAlO ₂ (0.50)	0.73*	350	Water (2.00)	19	Naphthalene (0.14) Tetralin (0.04)

* = Sodium naphthoate was used as the substrate.

occurred before or after decarboxylation. The sodium aluminate-catalyzed reaction of naphthoic acid in the water/tetralin system gave lower conversion (19%) than the reaction in water. It is clear that higher temperatures are required for better decarboxylation kinetics for this type of acid. Thus future work will be conducted at 385° and 400°C.

The CO/water reaction with sodium hydroxide in place of sodium aluminate gave lower conversions (9%) of acid at 300°C into naphthalene. Also, sodium hydroxide was added to the naphthoic acid to form sodium-1-naphthoate, and this salt was tested with sodium aluminate to give 12% and 19% conversions at 300° and 350°C, respectively. These reactions exhibit the lower reactivity of the carboxylate salt compared with the carboxylic acid form.

Besides catalyzing the decarboxylation of carboxylic acids, sodium aluminate may also have an effect on reactions of polyfunctional groups in the coal. The possibility also exists that the aluminate could moderate the alleged cross-linking effects during thermal treatments of coal. Therefore, carboxylic acids that have the potential for cross-linking or undergoing other reactions were investigated (Table 8).

In contrast to the reaction of naphthoic acid, the reaction of 2-phenoxybenzoic acid with CO-water at 350°C for 2 hr (no sodium aluminate) resulted in almost complete decarboxylation. The phenoxy group thus increases the decarboxylation reactivity of the acid group by an electronic substituent effect. The reaction was accompanied by a small amount of reduction of the diaryl ether linkage to give benzene and phenol. No products resulting from the addition of species derived from the carboxylate group to the adjacent ring to give a cyclic structure such as dibenzofuran or xanthone were observed. Thus no evidence for a cross-linking type of activity during decarboxylation could be obtained.

TABLE 8

CO/Water Reactions of Substituted Carboxylic Acids

Reaction Temp. = 350°C, Reaction Time = 2 hr Solvent (water) = 2 g, Reductant (CO) 1000 psi			
Catalyst (mmol/g Substrate)	Substrate (mmol)	Conversion (%)	Major Products (mmol)
None	2-PBA (2.37)	96	Benzene (0.05) Phenol (0.13) Diphenyl ether (1.82)
NaAlO ₂ (0.50)	2-PBA (2.27)	100	Phenol (2.37) Diphenyl ether (0.85)
None	2-BBA (2.40)	5	Diphenylmethane (0.11)
NaAlO ₂ (0.50)	2-BBA (2.29)	10	Diphenylmethane (0.22)

In the CO/water reaction of 2-phenoxybenzoic acid with added sodium aluminate, a large portion of the substrate underwent a hydrolysis reaction of the diaryl ether to give phenol as the major product. Since the hydrolysis reaction did not occur in the sodium aluminate-catalyzed reaction of diphenyl ether (see discussion above), the significant change in the reactivity of the ether oxygen could be attributed to the effect of the ortho-carboxylate group in the presence of sodium aluminate. Perhaps this effect results from the formation of a complex of the aluminate with the carboxylate that can catalyze the hydrolysis reaction. Again, no cyclic structures were found in the products.

The reaction of 2-benzylbenzoic acid with CO-water gave only 5% conversion of acid to diphenylmethane. Addition of sodium aluminate increased the conversion to 10%. Decarboxylation was slow for this substrate, but, as in the case of naphthoic acid, the addition of sodium aluminate improved the reactivity by a large factor. No cracking of the arylmethylene bond of the 2-benzylbenzoic acid occurred in these reactions, and only a trace of anthracene resulting from cyclization was found.

4.0 REFERENCES

1. Derbyshire, F. *ACS Div. of Fuel. Chem. Preprints* 1988, 33 (3), 188.
2. Garg, D.; Givens, E.N. *Fuel Proc. Technol.* 1984, 9, 29; Kovach, S.M.; Castle, L.J.; Bennett, J.V.; Svrodt, J.T. *Ind. Eng. Chem. Prod. Res. Dev.* 1978, 17, 62.
3. Mills, G.A.; Beodeker, E.R.; Oblad, A.G. *J. Amer. Chem. Soc.* 1950, 72, 1554.
4. Appell, H.R.; Wender, I.; Miller, R.D. *Prep. Pap.--Am. Chem. Soc., Div. of Fuel Chem.* 1969, 13, 39-44.
5. Sondreal, E.A.; Knudson, C.L.; Schiller, J.E.; May, T.H. *In Proceedings of the 9th Biennial Lignite Symp.: DOE/GFERC/IC-77/1*, 1977, pp 129-158.
6. Ross, D.S.; Green, R.K.; Monsani, R.; Hum, G.P. *Energy Fuels* 1987, 1, 287.
7. Jackson, W.R.; Lim, S.C.; Stray, G.J.; Larkins, F.P. *In Proceedings of the 1989 International Conference on Coal Science; Tokyo, Dec. 1989, Vol. II*, pp 815-818.
8. Hughes, C.P.; Sridhar, T.; Chuan, L.S.; Redlich, P.J.; Jackson, W.R.; Larkins, F.P. *USA/Australia Workshop on Use of Low-Rank Coals; Billings, MT, May 1991.*
9. Olson, E.S.; Sharma, R.K. "Semiannual Technical Progress Report for the Period July-December 1991," Energy and Environmental Research Center, 1991.
10. Jones, D.; Baltisberger, R.J.; Klabunde, K.J.; Woolsey, N.F.; Stenberg, V.I. *J. Org. Chem.* 1978, 43, 175-177.

11. Stenberg, V.I.; Wang, J.; Baltisberger, R.J.; Van Buren, R.; Woolsey, N.F. *J. Org. Chem.* **1978**, *43*, 2991-2994.
12. Matsen, F.A. *J. Chem. Phys.* **1956**, *24*, 602.
13. Becker, R.S.; Wentworth, W.E., *J. Am. Chem. Soc.* **1962**, *85*, 2210-2214.
14. Hedges, R.M.; Matsen, F.A. *J. Chem. Phys.* **1958**, *28*, 950.
15. Chilton, H.T.J.; Gowenlock, B.G. *Trans. Faraday Soc.* **1954**, *50*.
16. Levanon, H.; Neta, P.; Trozzolo, A.M. In *Organic Free Radicals*. ACS Symp. Series 69; Pryor, W.A., ed.; Amer. Chem. Soc. Washington D.C., 1978, pp. 401-409.
17. Pross, A. *Acc. Chem Res.* **1985**, *18*, 212-219.
18. Morris, R.M.; Kaba, R.A.; Groshens, T.G.; Klabunde, K.J.; Baltisberger, R.J.; Woolsey, N.F.; Stenberg, V.I. *J. Amer. Chem. Soc.* **1980**, *102*, 3419-3424.
19. Guglielminotti, E.; Coluccia, S.; Garrone, E.; Cerruti, L.; Zecchina, A. *J. Chem. Soc. Faraday Trans.* **1979**, *1*, 96.
20. Stenberg, V.I.; Baltisberger, R.J.; Knittal, D.; Wettlaufer, D.; Woolsey, N.F.; Knudsen, C. 14th Intersociety Confr., Aug 5-10, 1979, Boston, MA.
21. Stenberg, V.I.; Baltisberger, R.J.; Klabunde, K.J.; Woolsey, N.F.; Severson, D.; Souby, M. "Quarterly Technical Progress report for the Period July-September 1978," Contract No. EX-76-C-01-2211.

U.S. DEPARTMENT OF ENERGY
FEDERAL ASSISTANCE MANAGEMENT SUMMARY REPORT

1. Program/Project Identification No. DE-FC21-86MC10837	2. Program/Project Title Liquefaction Reactivity of Low-Rank Coals (3.4)	3. Reporting Period 3-1-92 through 6-30-92
4. Name and Address Energy and Environmental Research Center University of North Dakota Box 8213, University Station, Grand Forks, ND 58202 (701) 777-5000		5. Program/Project Start Date 4-1-86
		6. Completion Date 9-30-92

7. FY 91/92	8. Months or Quarters Quarters	1991						1992					
		JUL	AUG	SEP	OCT	NOV	DEC	JAN	FEB	MAR	APR	MAY	JUN
9. Cost Status	a. Dollars Expressed in Thousands	b. Dollar Scale											
10. Cost Chart													
Fund Source		Quarter				Cum. to Date	Tot. Plan						
		1st	2nd	3rd	4th								
DOE	P	37	37	37	36	147	147						
	A	27	22	24	23	96							
	P												
	A												
	P												
	A												
	P												
	A												
Total P		37	37	37	36	147	147						
Total A		27	22	24	23	96							
Variance		10	15	13	13	51							
P = Planned A = Actual		c. Cumulative Accrued Costs											
Total Planned Costs for Program/Project \$147		Planned		37			74			111			147
		Actual		27			49			73			96
		Variance		10			25			38			51

11. Major Milestone Status	Units Planned	
	Units Complete	
Task 1:		
A. Testing Aluminates with Low-Rank Coal	P	1 ▽ 2 ▽ 3 ▽ 4 ▽ 5 Δ
	C	
	P	
	C	
B. Testing of Heteropolymers	P	1 ▽ 2 ▽ 3 Δ
	C	
	P	
	C	
C. Testing with Colloidal Coal	P	1 Δ
	C	
	P	
	C	
D. Mechanism Studies	P	1 ▽ 2 Δ
	C	
	P	
	C	
	P	
	C	
	P	
	C	
	P	
	C	
	P	
	C	

12. Remarks
Due to EERC fiscal year end, the June books do not close until July 25, 1992. Costs posted through July 8 have been included.

13. Signature of Recipient and Date
Chun S. Olson 7-30-92

14. Signature of DOE Reviewing Representative and Date

U.S. DEPARTMENT OF ENERGY
FEDERAL ASSISTANCE MANAGEMENT SUMMARY REPORT

1. Program/Project Identification No. DE-FC21-86MC10837		2. Program/Project Title Liquefaction Reactivity of Low-Rank Coals (3.4)		3. Reporting Period 3-1-92 through 6-30-92	
4. Name and Address Energy and Environmental Research Center University of North Dakota Box 8213, University Station Grand Forks, ND 58202 (701) 777-5000				5. Program/Project Start Date 4-1-86	
				6. Completion Date 9-30-92	
Milestone ID. No.	Description	Planned Completion Date	Actual Completion Date	Comments	
Task 1					
A.	Testing Aluminates with Low-Rank Coal:				
1.	Effects of pH	9-30-91	12-31-91		
2.	Effects of concentration	10-31-92			
3.	Effects of temperature	11-30-91	3-31-92		
4.	Effects of catalyst aging	1-31-92			
5.	Reuse of water/aluminate	2-29-92			
B.	Testing of Heteropolymers:				
1.	Aluminum with phosphorus	3-31-92			
2.	Aluminum with silicon or aluminum with titanium	4-30-92			
3.	Aluminum with other metals	6-30-92			
C.	Testing with Colloidal Coal	12-31-91			
D.	Mechanism Studies:				
1.	Extent of decarboxylation	1-31-92	3-31-92		
2.	Model compound tests	5-31-92	6-30-92		
Task 2	Final Project Report	8-31-92			